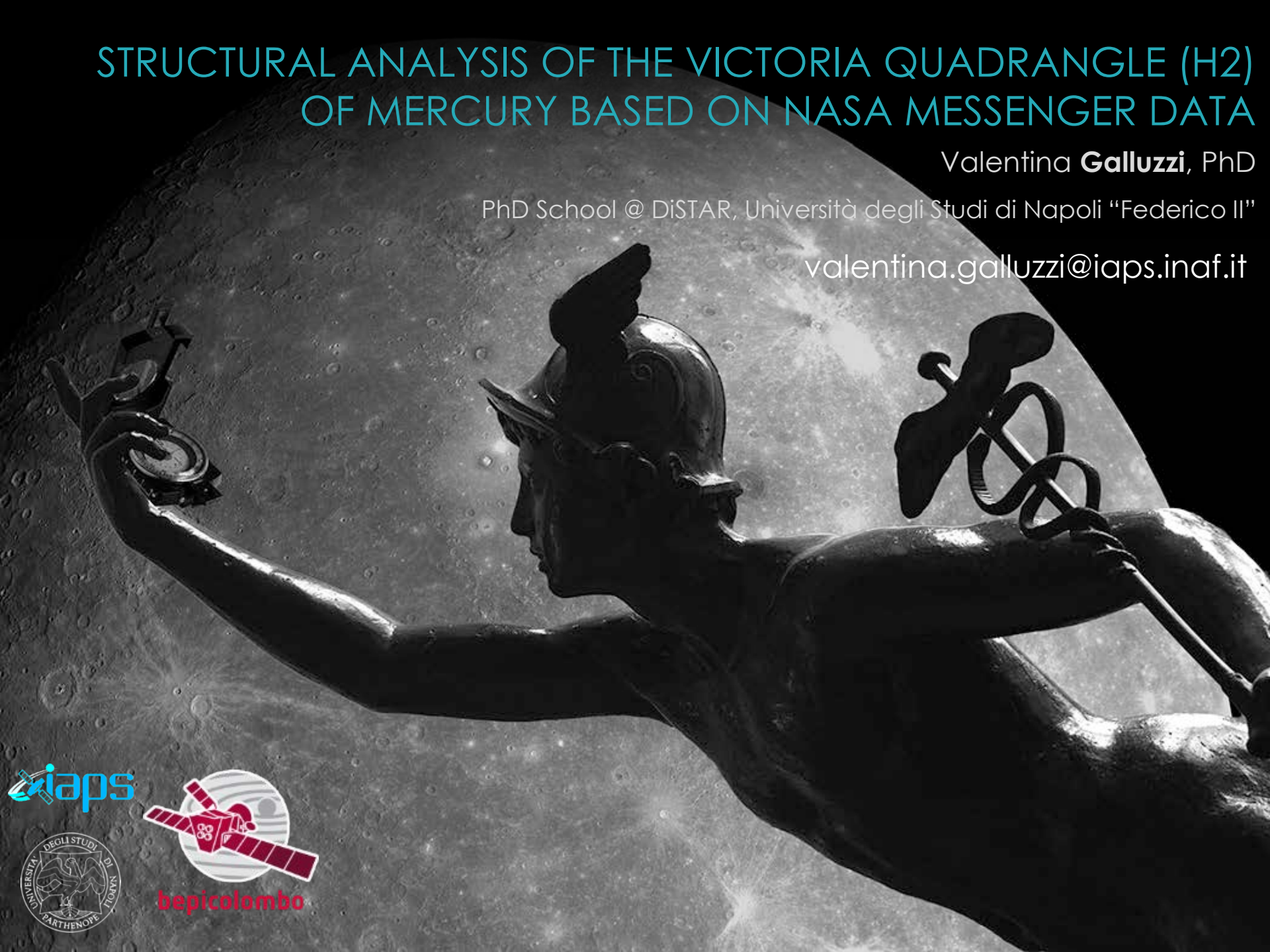


# STRUCTURAL ANALYSIS OF THE VICTORIA QUADRANGLE (H2) OF MERCURY BASED ON NASA MESSENGER DATA

Valentina **Galluzzi**, PhD

PhD School @ DiSTAR, Università degli Studi di Napoli “Federico II”

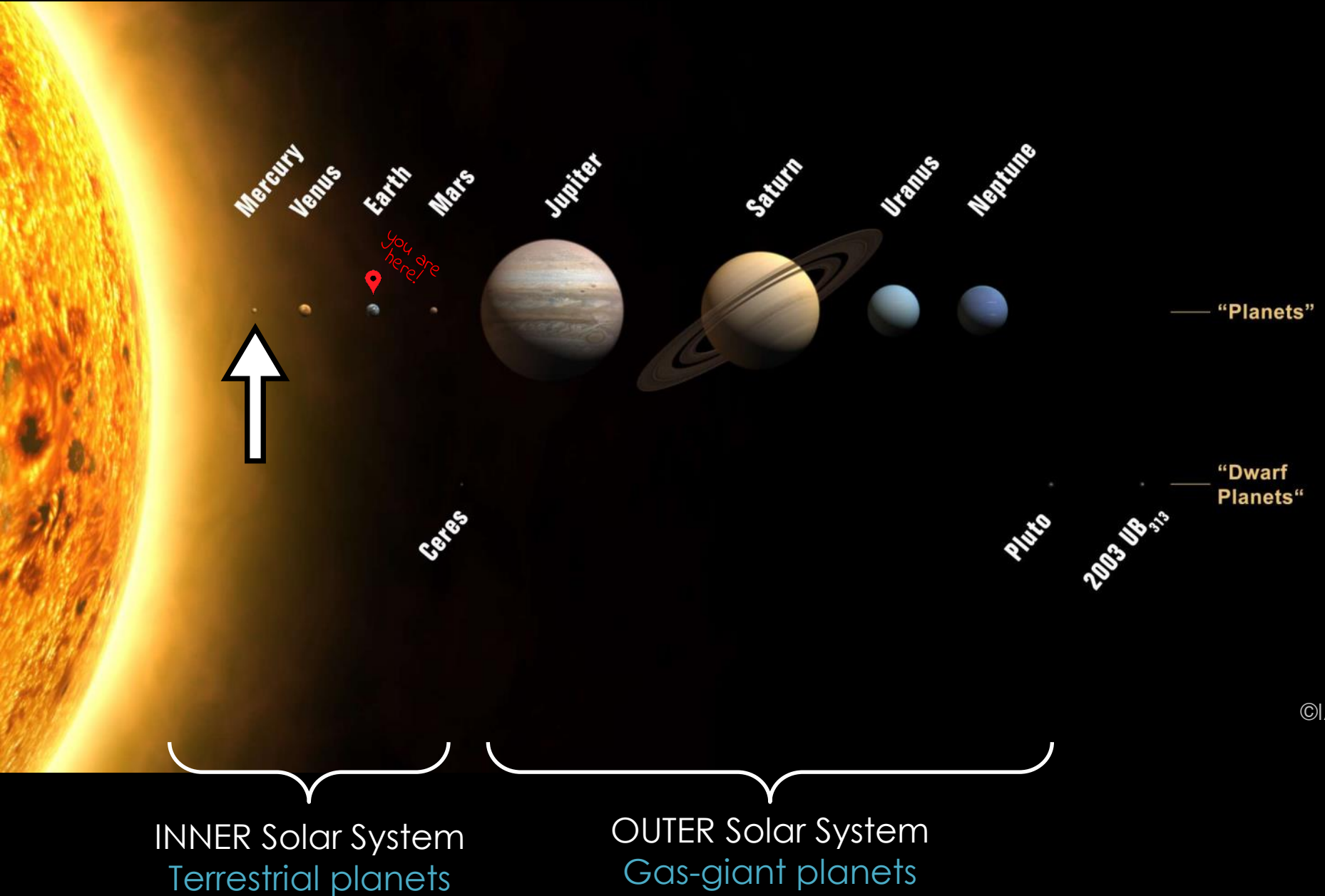
[valentina.galluzzi@iaps.inaf.it](mailto:valentina.galluzzi@iaps.inaf.it)



bepicolombo

*Objective of this work is the **mapping** and **structural analysis** of the Victoria quadrangle and a reconnaissance study of the **geometry** and **kinematics** of lobate scarps on **Mercury.***





MOON



MERCURY



EARTH



**Radius**

**1738** Km

**Density**

**3.35** g/cm<sup>3</sup>

**Gravity**

**0.17** g

**2440** Km

**5.42** g/cm<sup>3</sup>

**0.38** g

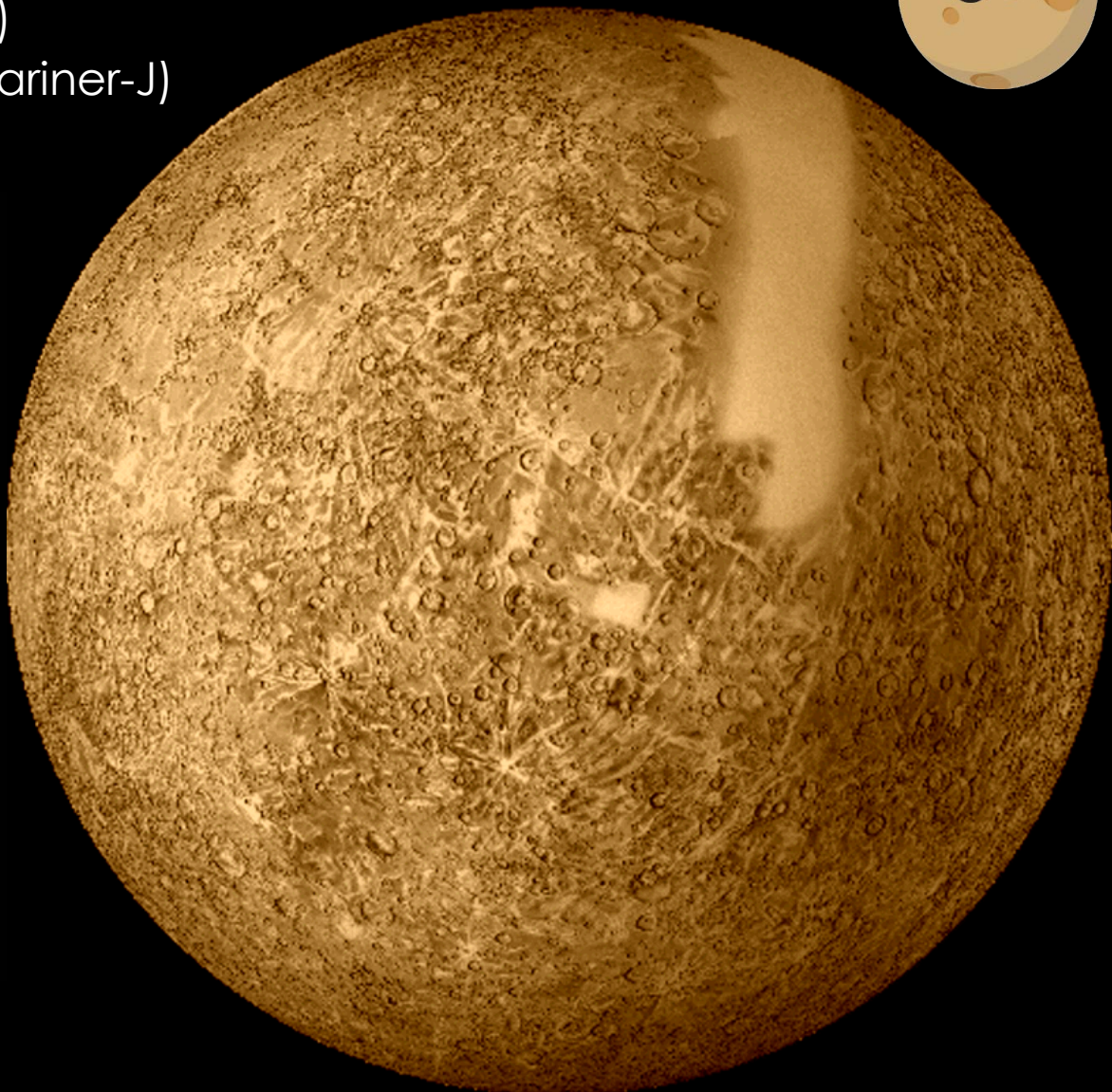
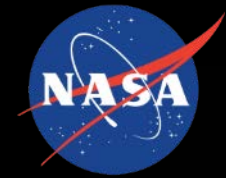
**6378** Km

**5.52** g/cm<sup>3</sup>

**1.00** g

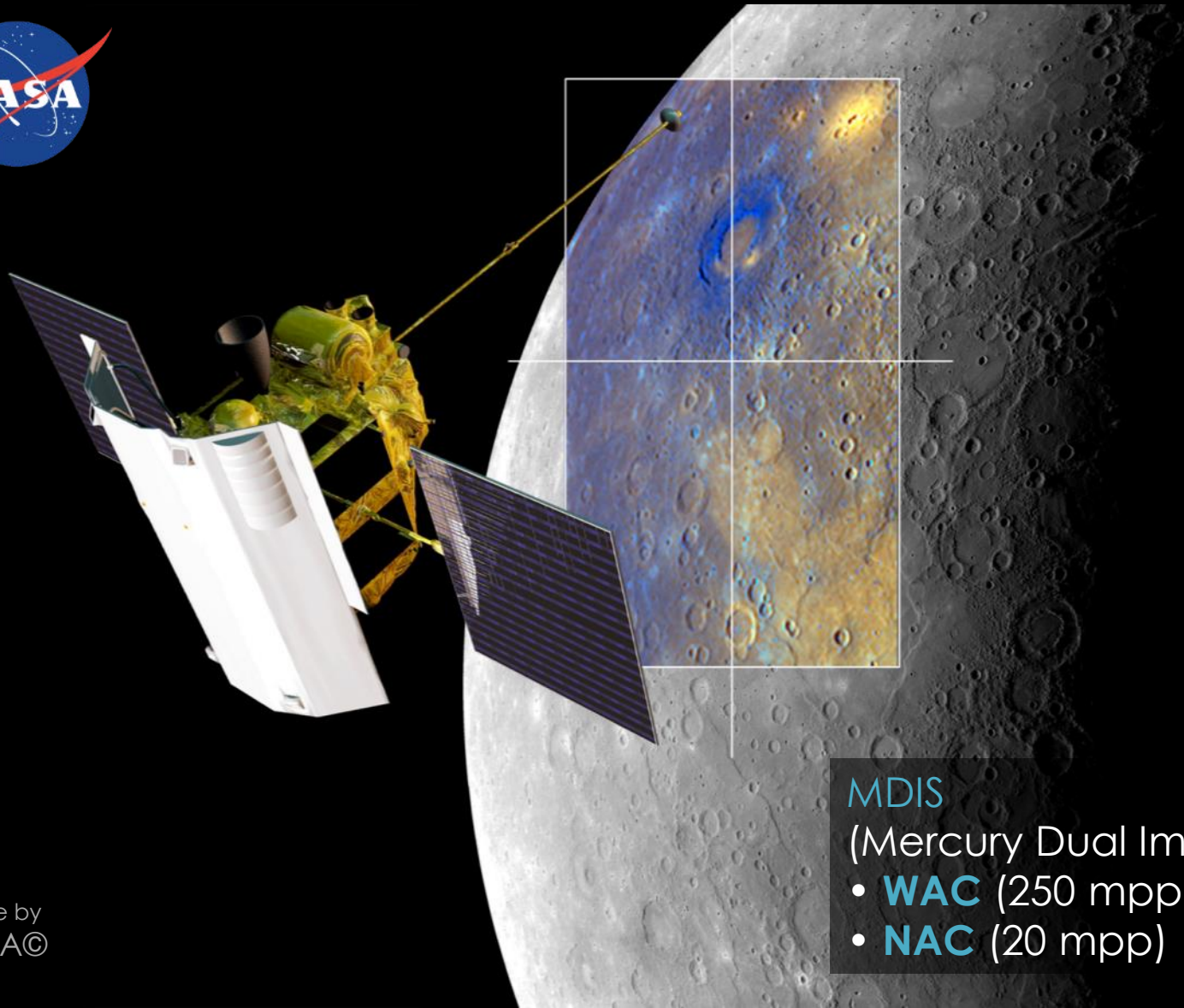


1973 – 1975 – Mariner 10 (NASA)  
(Mariner Venus/Mercury 73 – Mariner-J)





## 2004 – 2015 – MESSENGER (NASA) (MErcury Surface ENvironment, GEochemistry and Ranging)



### MDIS

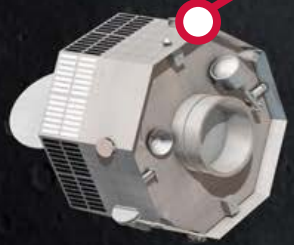
(Mercury Dual Imaging System)

- **WAC** (250 mpp)
- **NAC** (20 mpp)

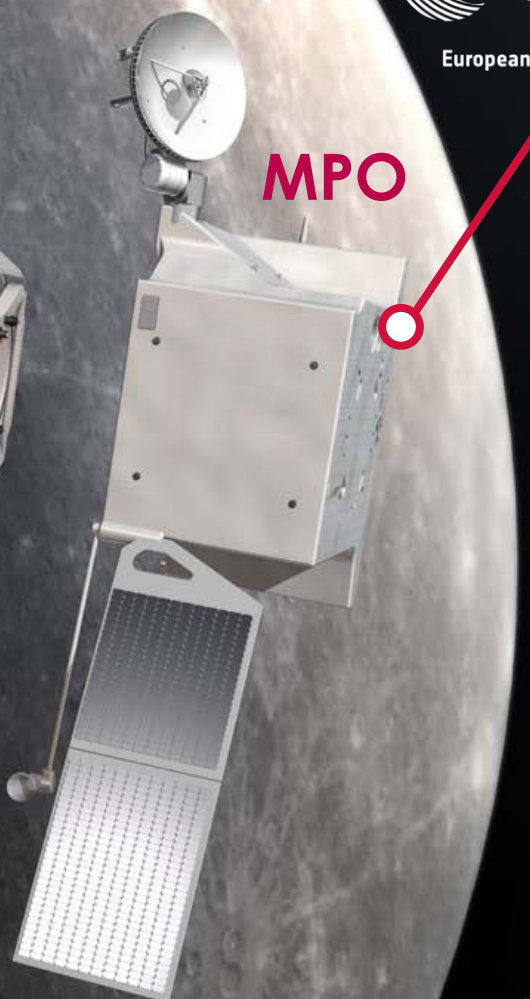


esa  
European Space Agency

MMO



MPO



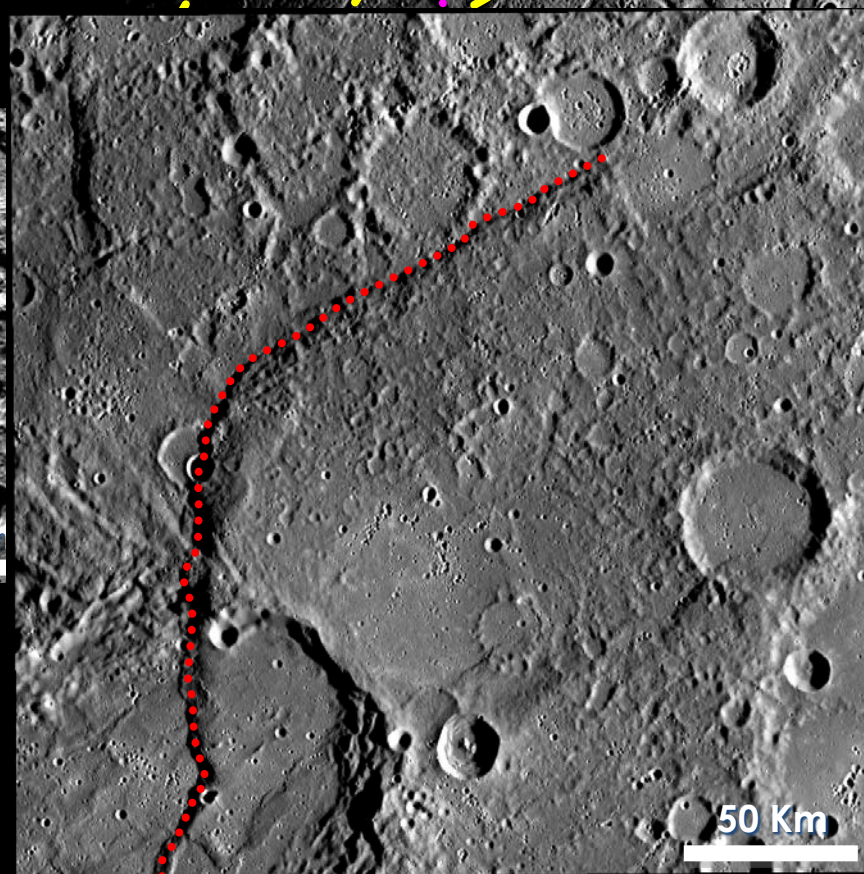
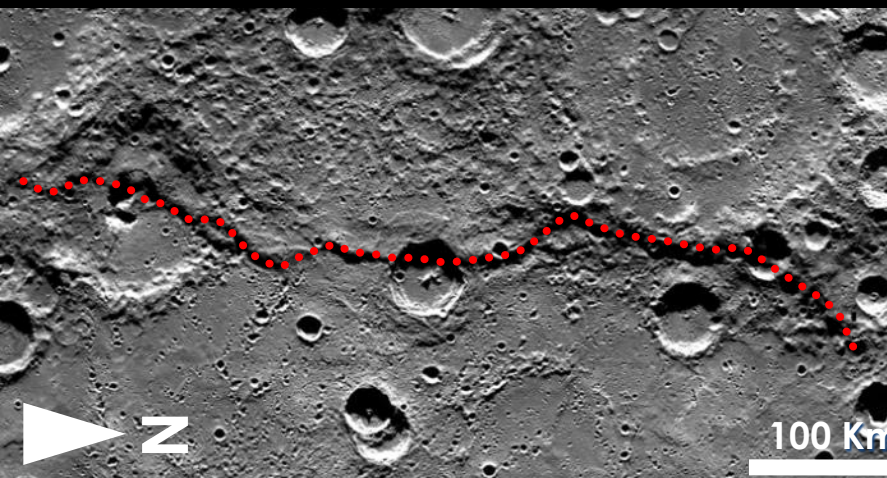
2017



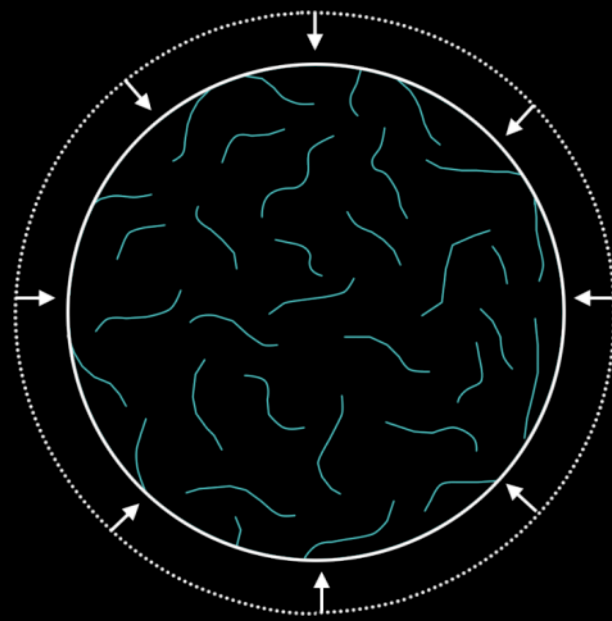
bepicolombo

JAXA

- EXTENSION structures
  - radial GRABEN
  - concentric GRABEN
- COMPRESSION structures
  - WRINKLE RIDGES (*thrusts?*)
- COMPRESSION structures (outside craters)
  - LOBATE SCARPS (*thrusts*)



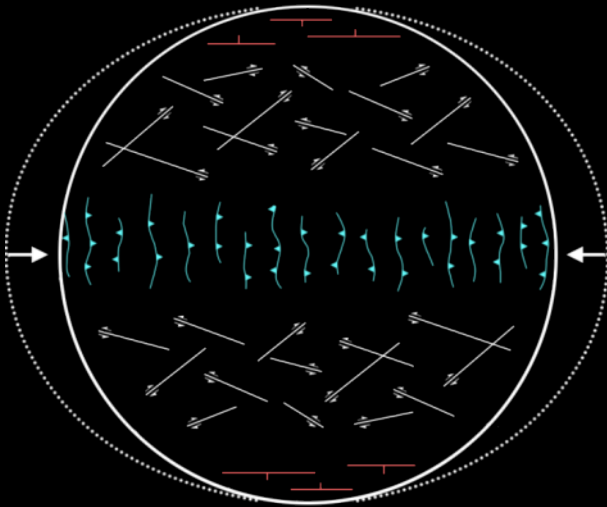
Strom et al., 1975



### global contraction

(Strom, 1975)

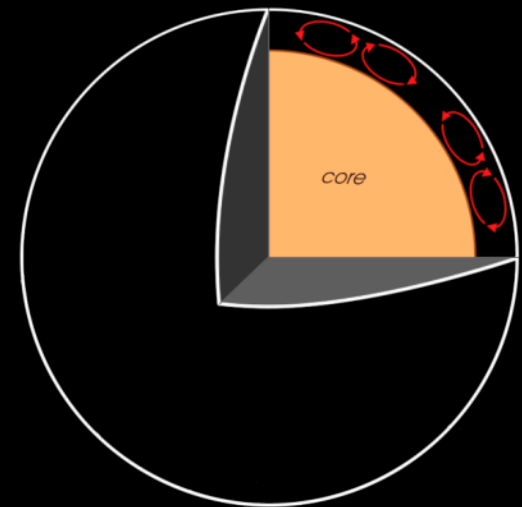
- ↓ core solidification
- ↓ surface shrinking
- ubiquitous thrusts
- random orientations



### tidal despinning

(Melosh & Dzurisin, 1978)

- ↓ rotation despinning
- ↓ inversion tectonics
- all kind of faults
- latitudinal variations

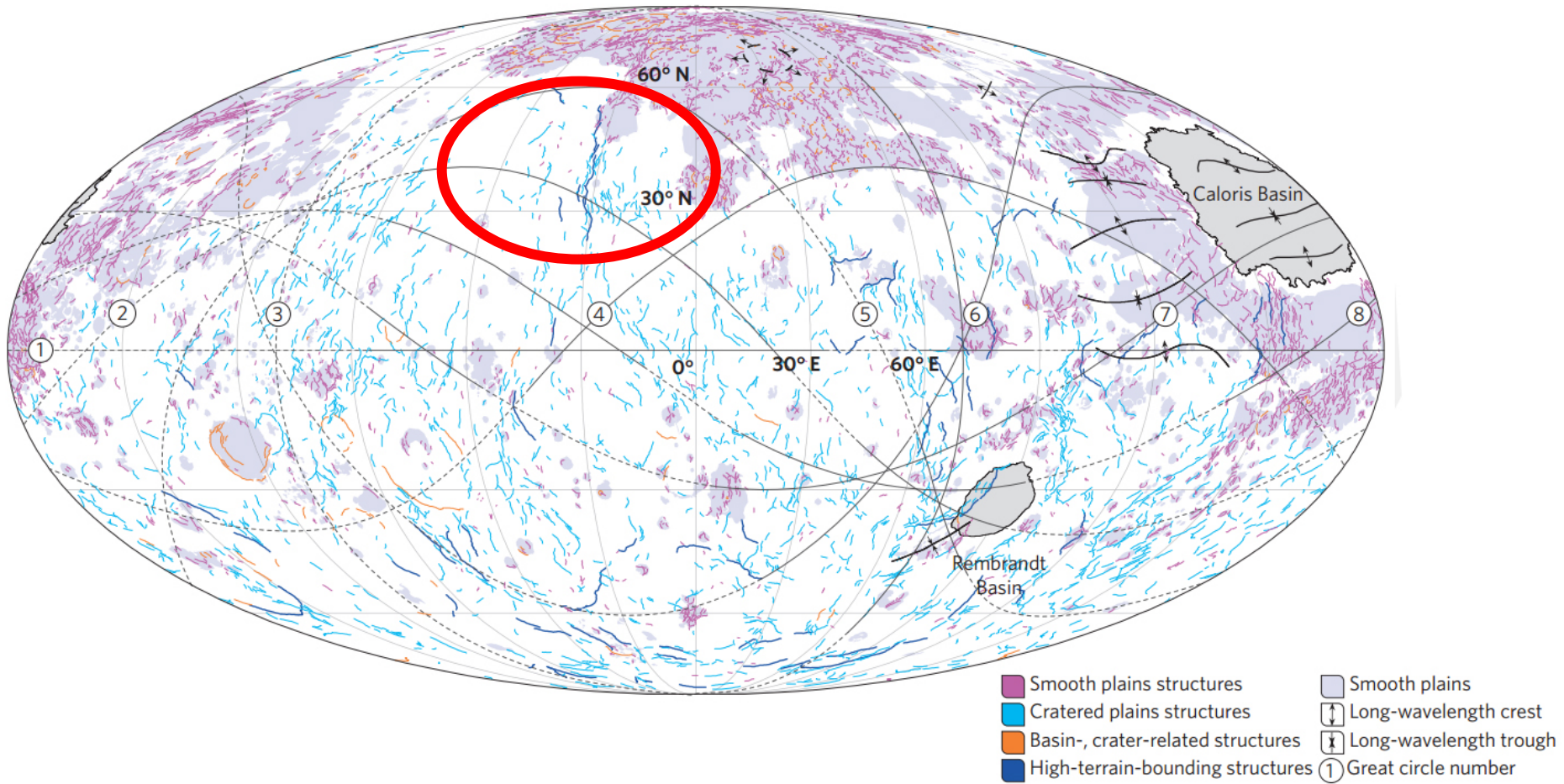


### mantle convection

(King, 2008)

- ↓ convective cells...
- ...changing over time

# Global structural map



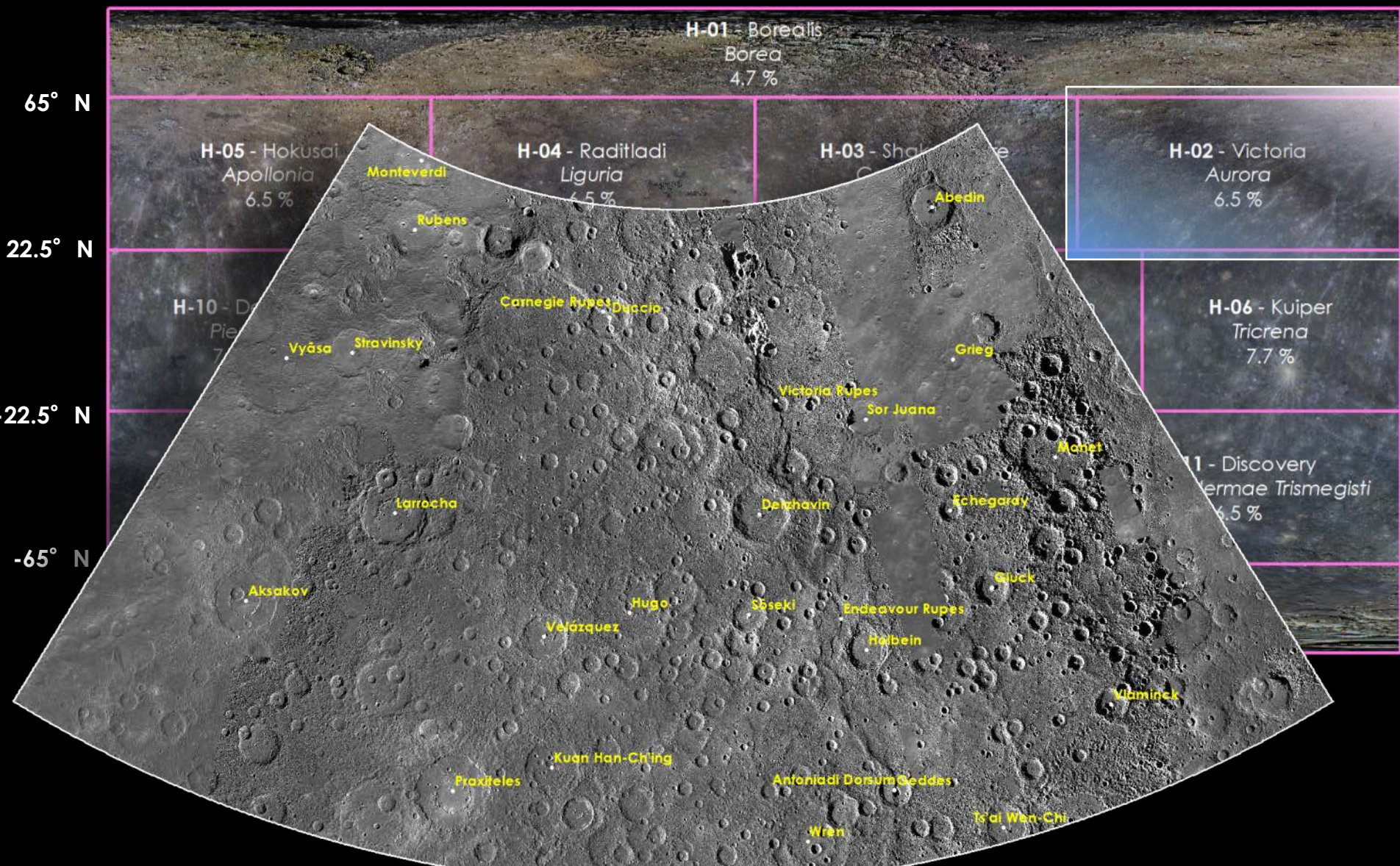
0°

90° E

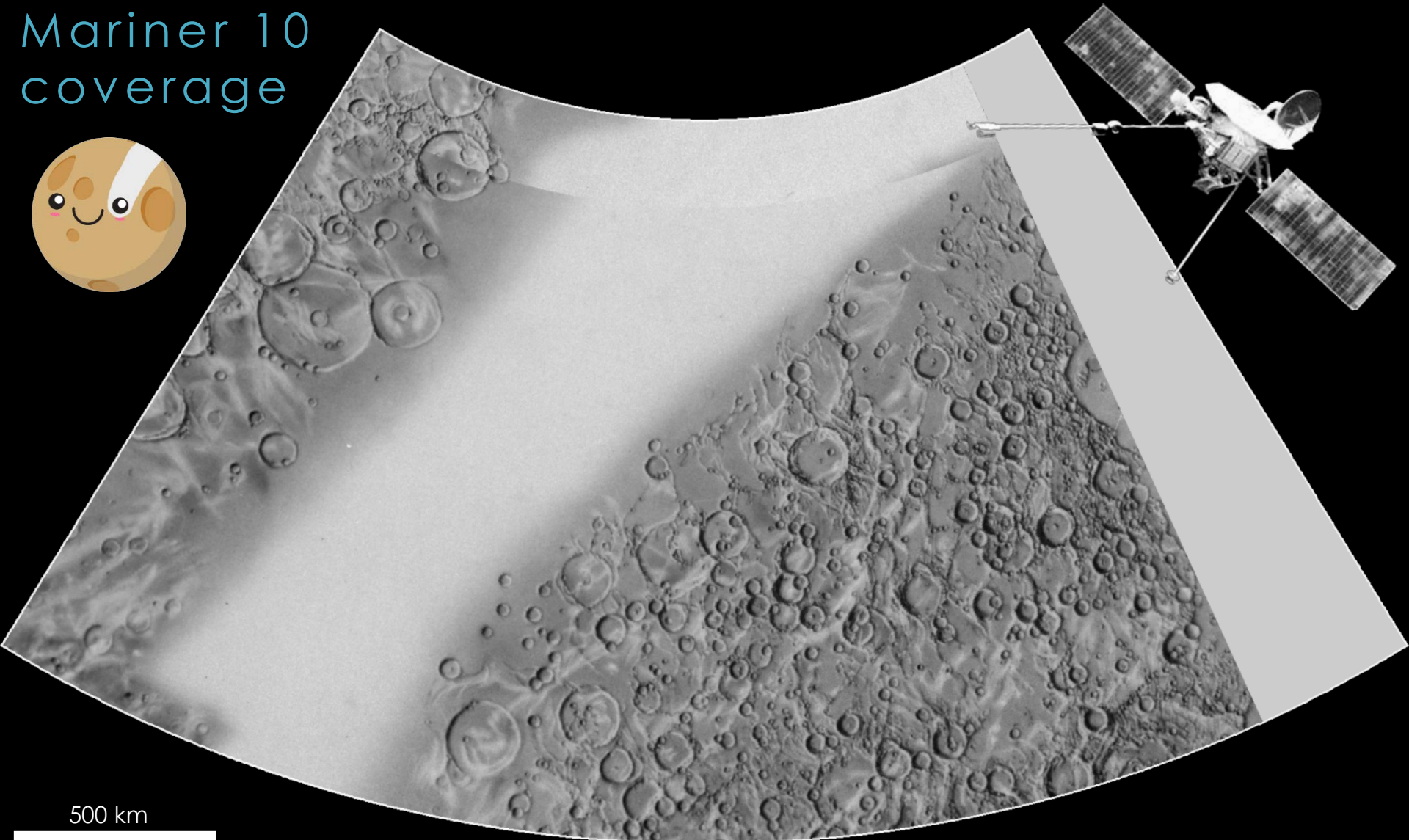
180° E

270° E

360° E



# Mariner 10 coverage



500 km

BASEMAP  
Airbrush\_shadedrelief  
© NASA

# Mariner 10 geology

1:5M

McGill & King (1983)

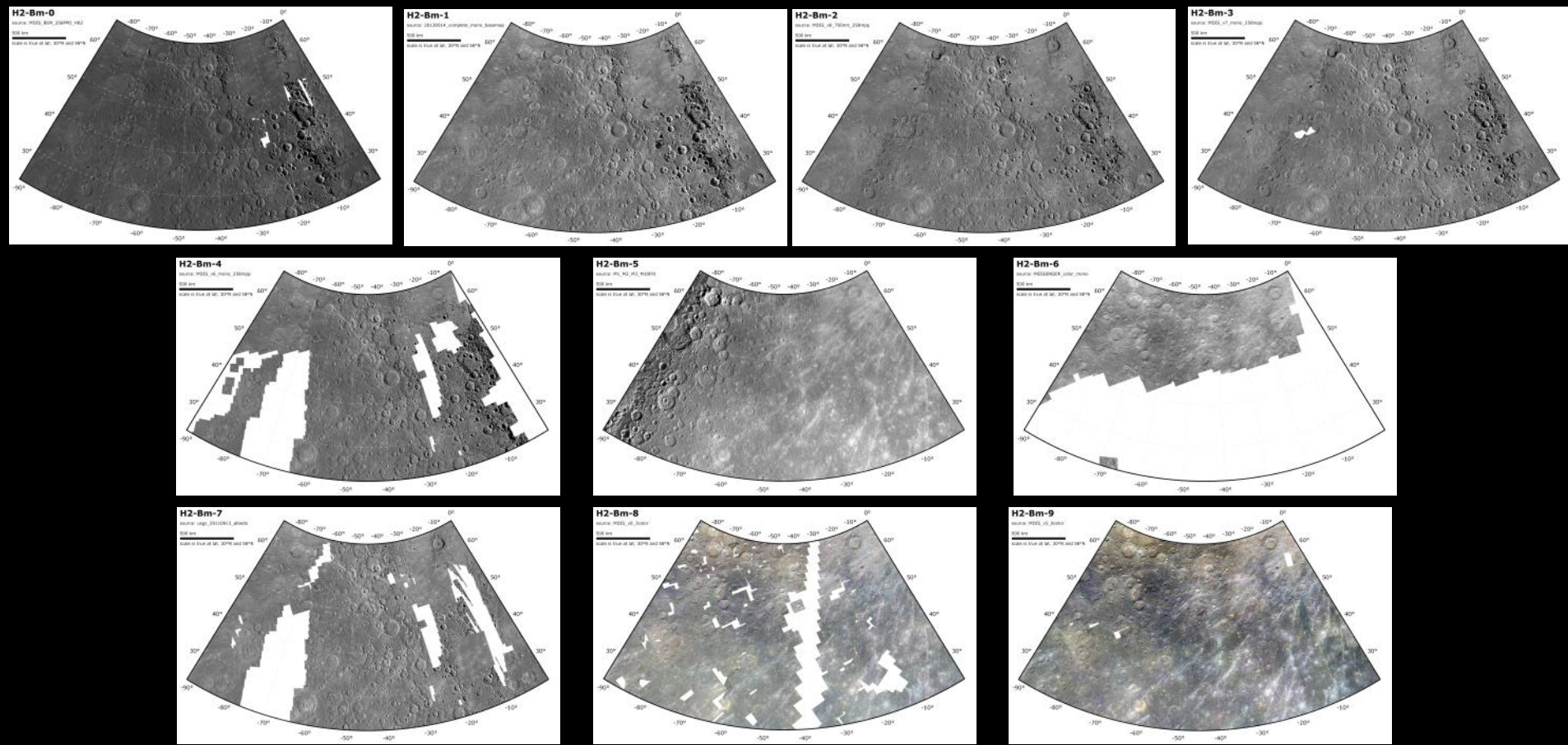
64%  
unmapped

500 km

BASEMAP  
Airbrush\_shadedrelief  
© NASA



# MESSENGER BASEMAPS



# BDR tiles

risoluzione: 256 ppx  
~ 166 mpp

low emission angles

moderate/high  
incidence angles

NAC + WAC-G

MDIS\_BDR\_256PPD\_H02NW0

MDIS\_BDR\_256PPD\_H02NE0

MDIS\_BDR\_256PPD\_H02SE0

MDIS\_BDR\_256PPD\_H02SW0

500 km

BASEMAP  
mdis\_bdr\_256ppd\_H02  
© NASA / JHUAPL / CIW

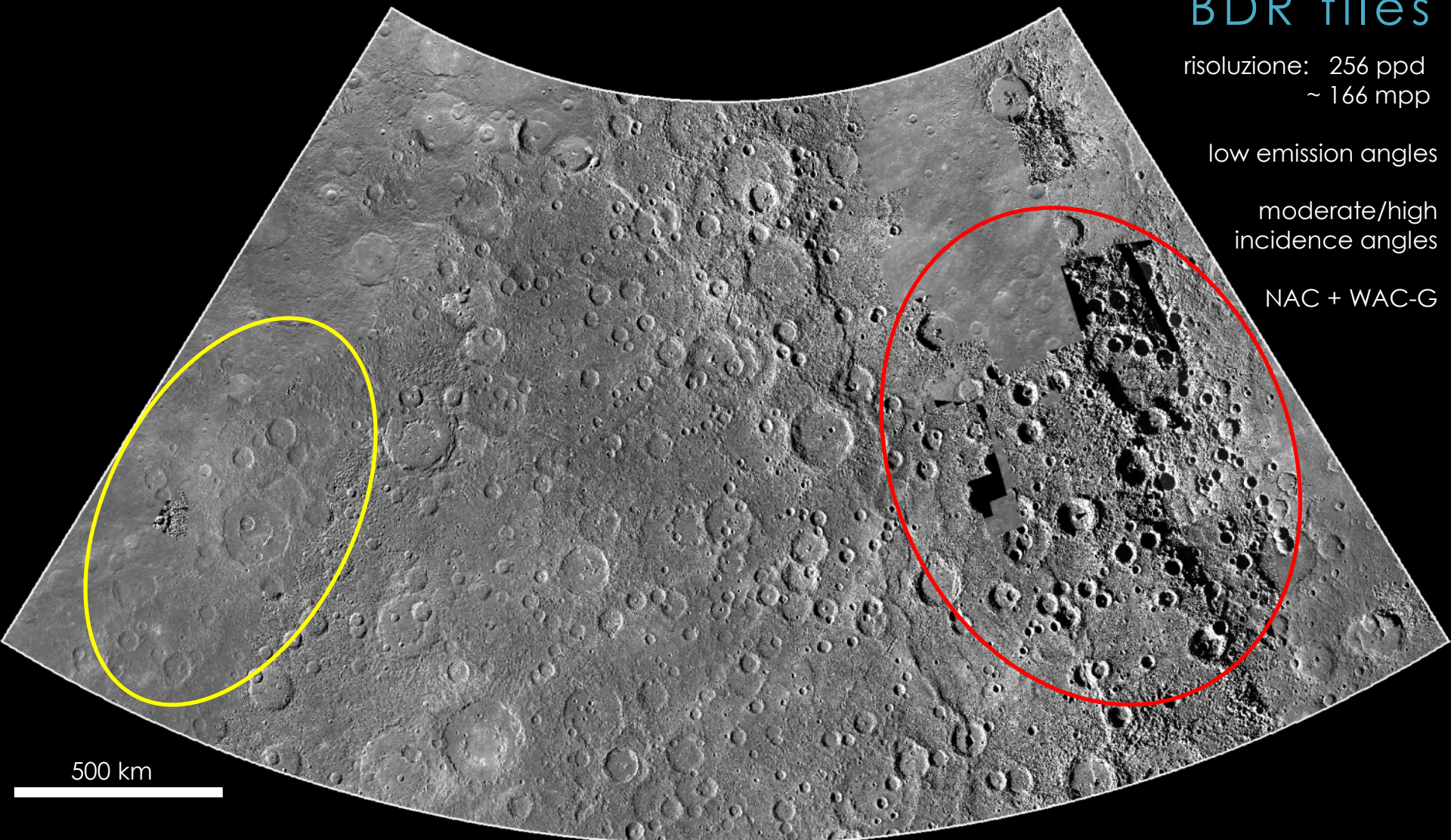
# BDR tiles

risoluzione: 256 ppd  
~ 166 mpp

low emission angles

moderate/high  
incidence angles

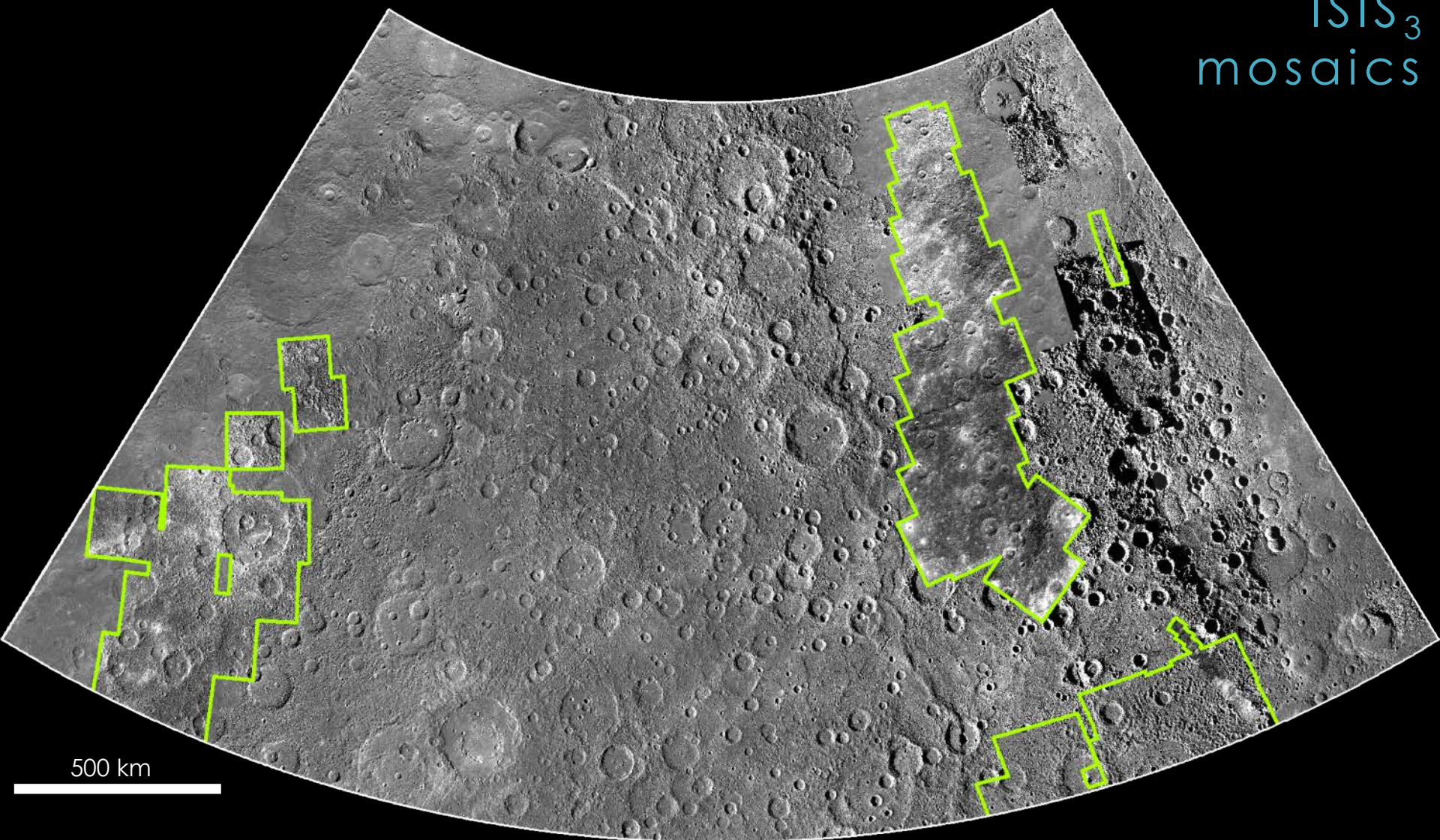
NAC + WAC-G



500 km

BASEMAP  
mdis\_bdr\_256ppd\_H02  
© NASA / JHUAPL / CIW

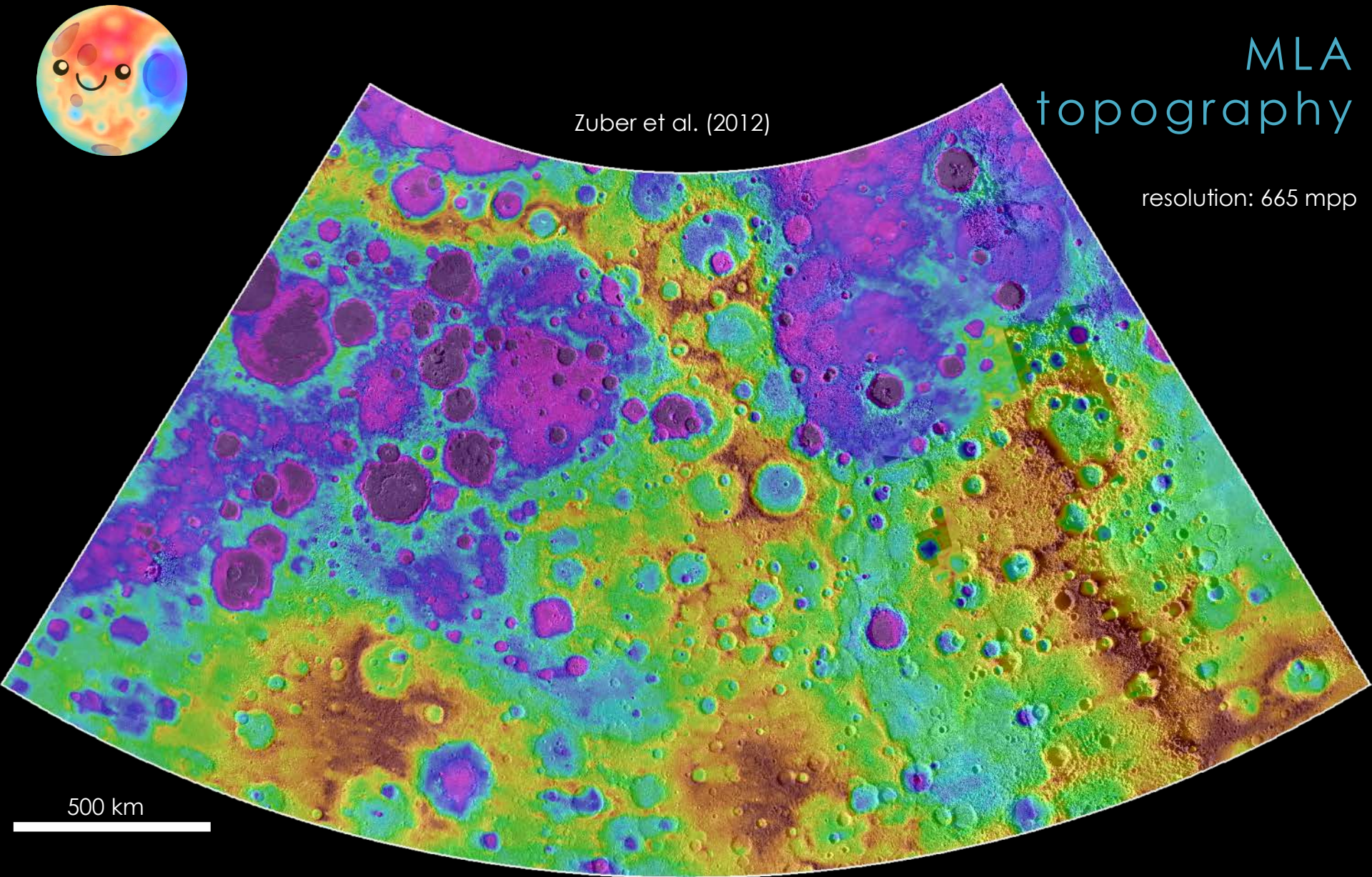
ISIS<sub>3</sub>  
mosaics



500 km

BASEMAP  
mdis\_bdr\_256ppd\_H02  
© NASA / JHUAPL / CIW

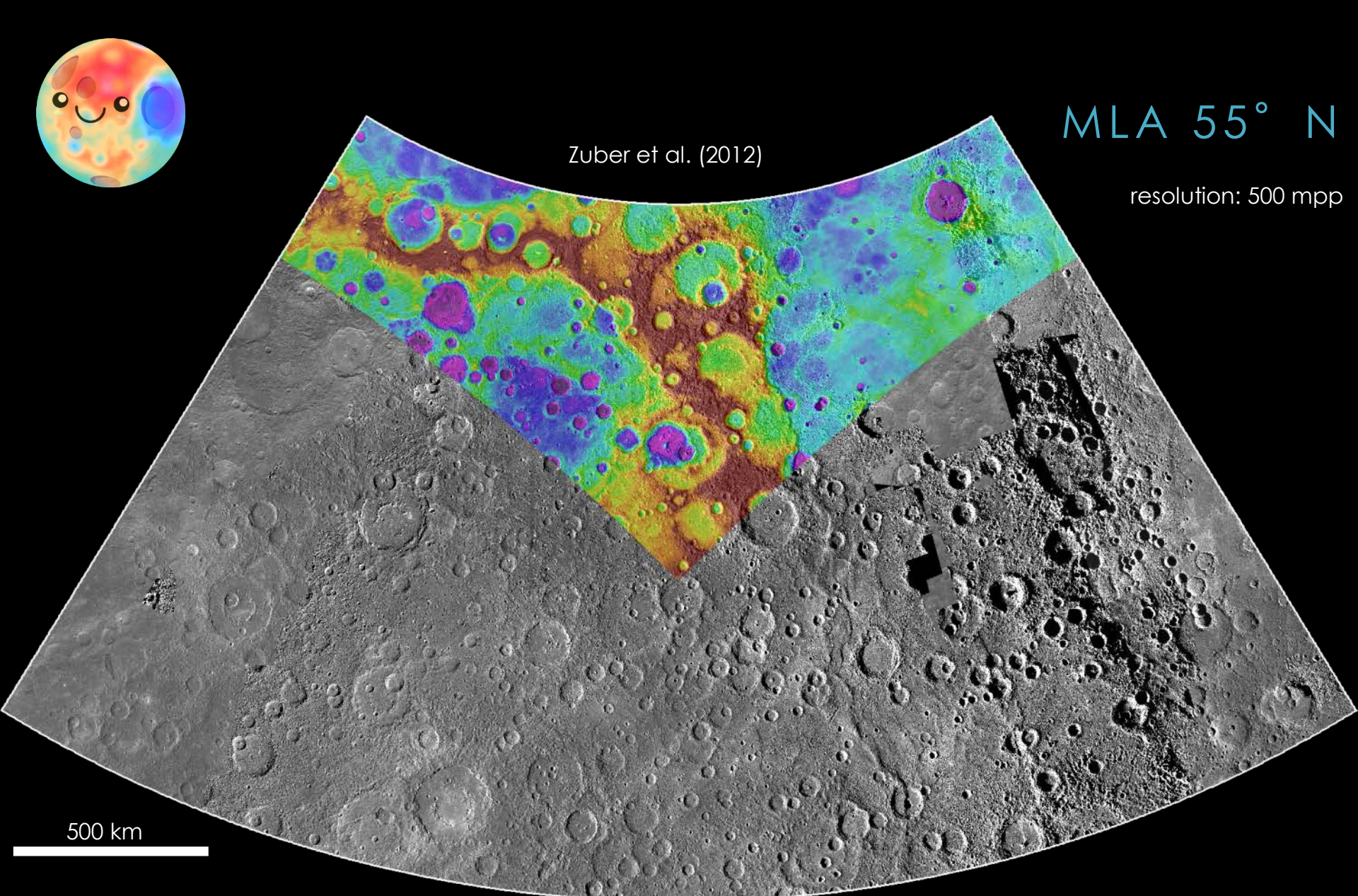
# MLA topography



500 km

TOPOGRAPHY  
hdem\_64  
© NASA

BASEMAP  
mdis\_bdr\_256ppd\_H02  
© NASA / JHUAPL / CIW



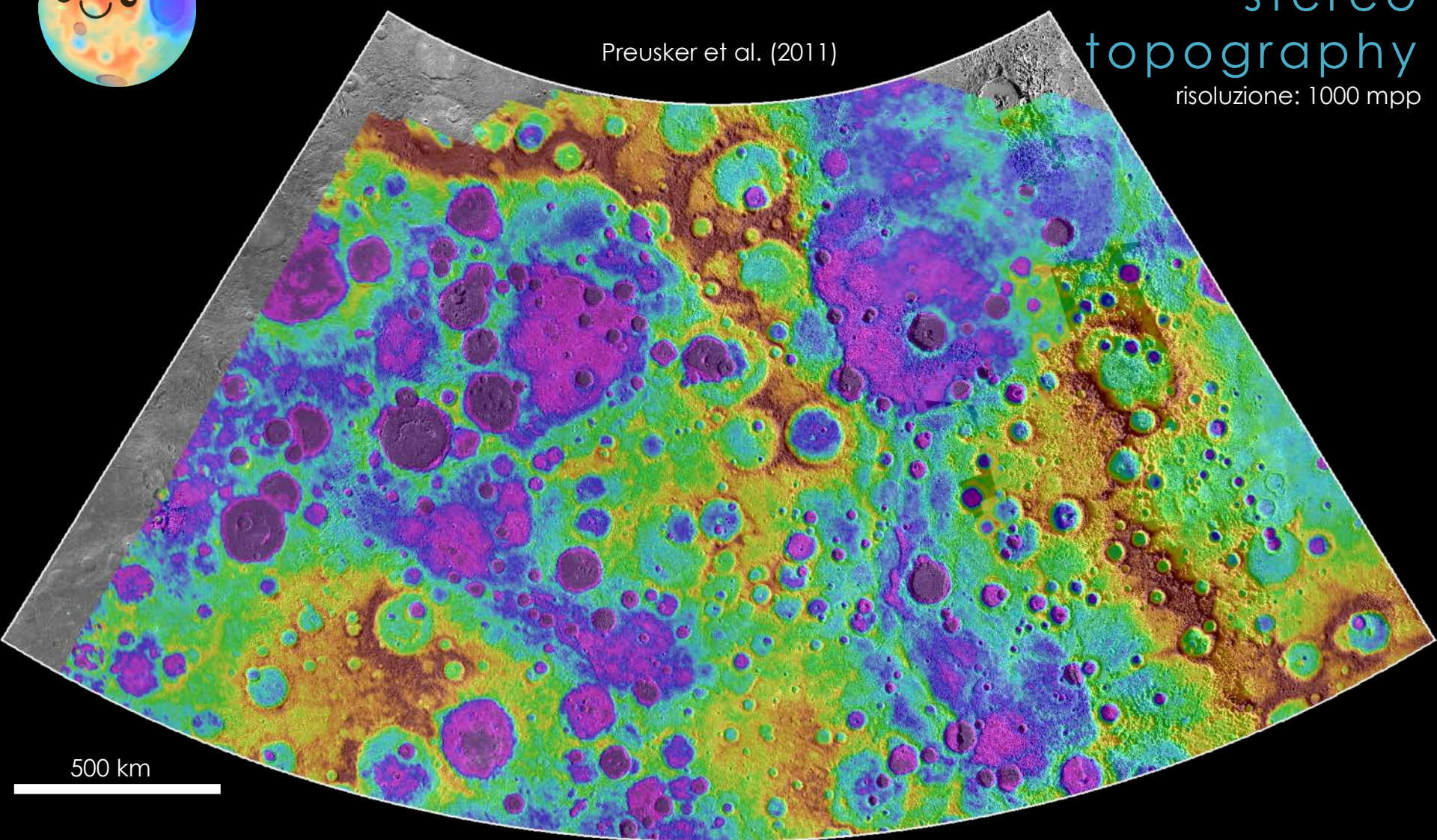
TOPOGRAPHY  
hdem\_55n\_500m  
© NASA

BASEMAP  
mdis\_bdr\_256ppd\_H02  
© NASA / JHUAPL / CIW



Preusker et al. (2011)

stereo  
topography  
risoluzione: 1000 mpp



500 km

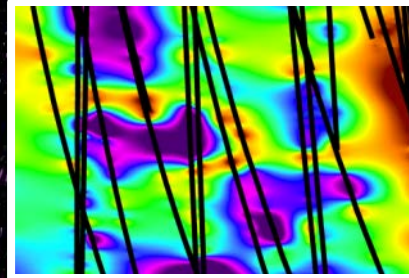
TOPOGRAPHY  
M2\_equi000\_1km  
© DLR

BASEMAP  
mdis\_bdr\_256ppd\_H02  
© NASA / JHUAPL / CIW

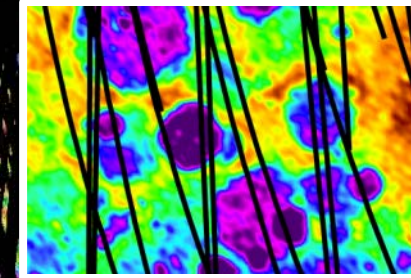


MLA tracks

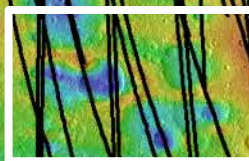
MLA



stereo



500 km



TOPOGRAPHY  
hdem\_64  
© NASA

BASEMAP  
mdis\_bdr\_256ppd\_H02  
© NASA / JHUAPL / CIW

# METHODS

planetary geological mapping

planetary surface dating

fault slip data of remote sensed structures

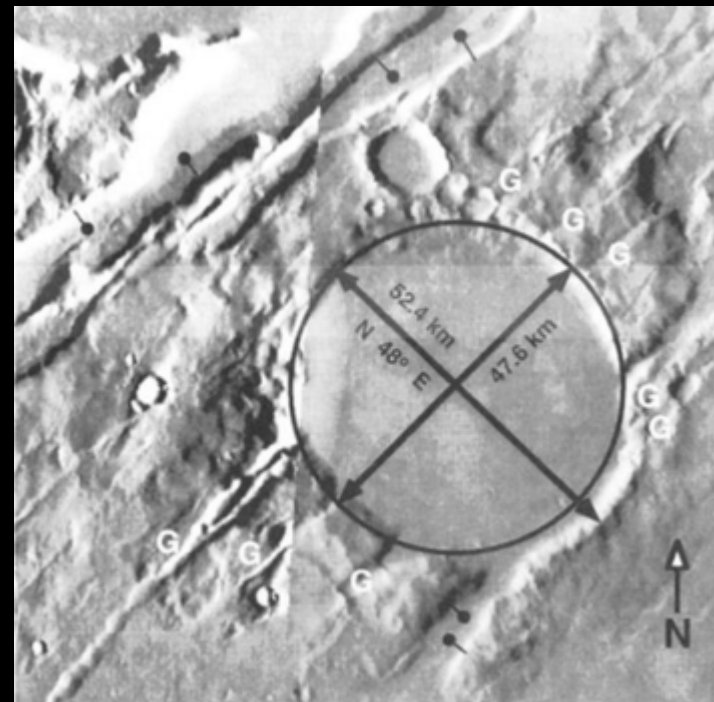


Amenthes Rupes (Mars)  
from **Watters (1993)**

♀ Past studies already considered **faulted craters** as an important **marker** to constrain the nature of **faults** on terrestrial planets ... **QUALITATIVE approach**  
e.g. Strom et al. (1975); Watters (1993); Watters et al. (1998)

DIP-SLIP  
motion

unknown  
dip-angle



Gandzani Crater, Tempe Terra (Mars)  
from **Golombek et al. (1996)**

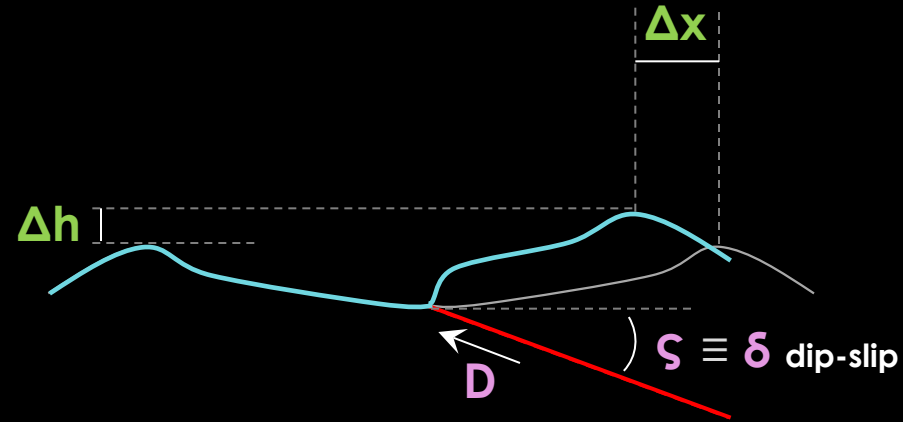
♀ ... or even to perform **strain analysis**:  
e.g. Thomas & Allemand (1993); Golombek et al.  
(1996); Pappalardo & Collins (2005)

**QUANTITATIVE approach**

♀ The analysis of faulted craters leads to assess:

**Δx** slip **horizontal** component

**Δh** slip **vertical** component



♀ Thus these parameters can be calculated:

**Σ** slip **plunge**

**δ** fault **true dip**

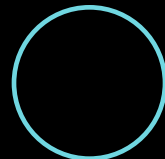
**λ** fault **rake**

**D** fault **displacement**

$$\Sigma = \tan^{-1}(\Delta h / \Delta x) \quad \delta = \tan^{-1}(\tan \Sigma / \sin \Phi) \quad \lambda = \cos^{-1} (\text{strike} \cdot \text{slip}) \quad D = \Delta h / \sin \Sigma$$

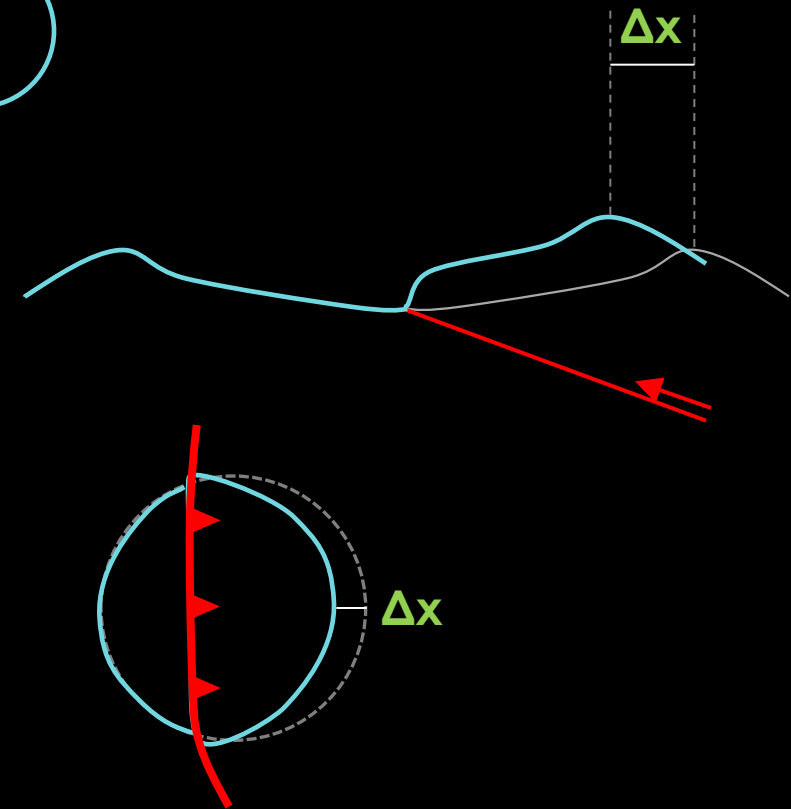
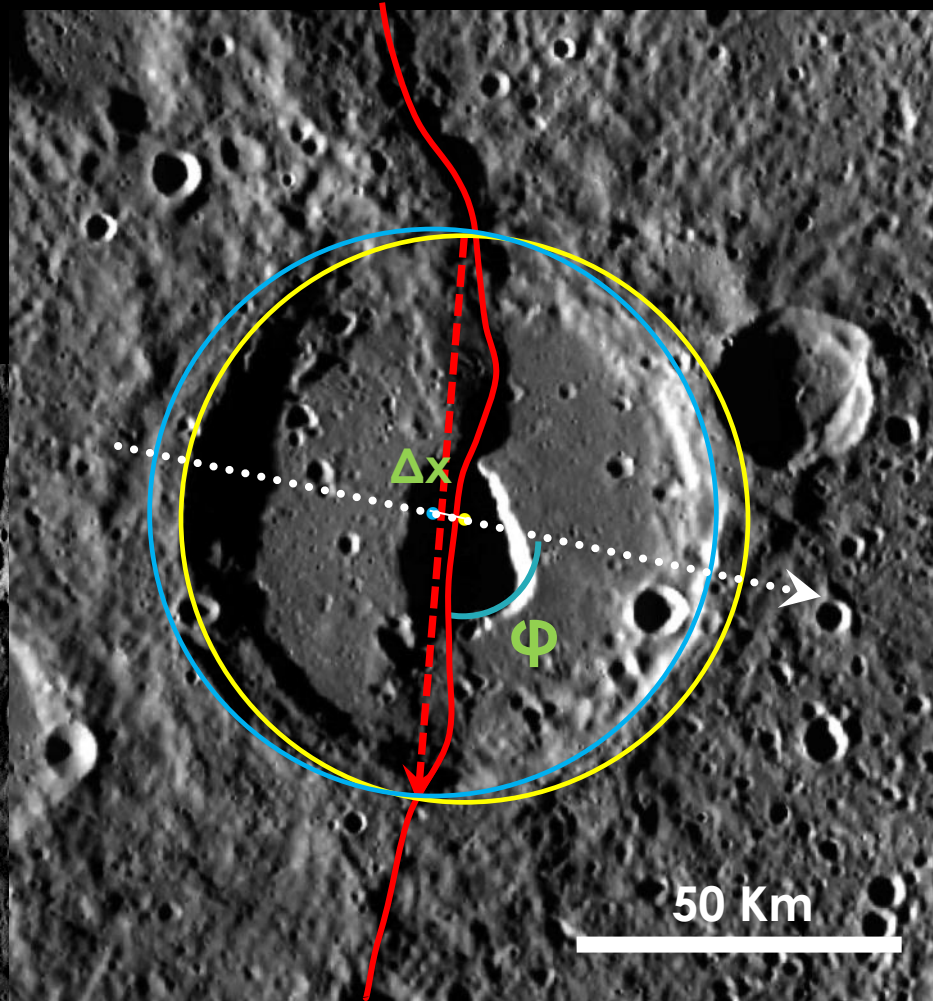
## ♀ ASSUMPTION:

The crater was originally **circular** in shape



$\Delta x$

## STEREOGRAPHIC PROJECTION !!



$\Delta x$  segment also indicates the **slip's trend**

$$\Phi = 90^\circ$$

→

dip-slip

$$\Phi \neq 90^\circ$$

→

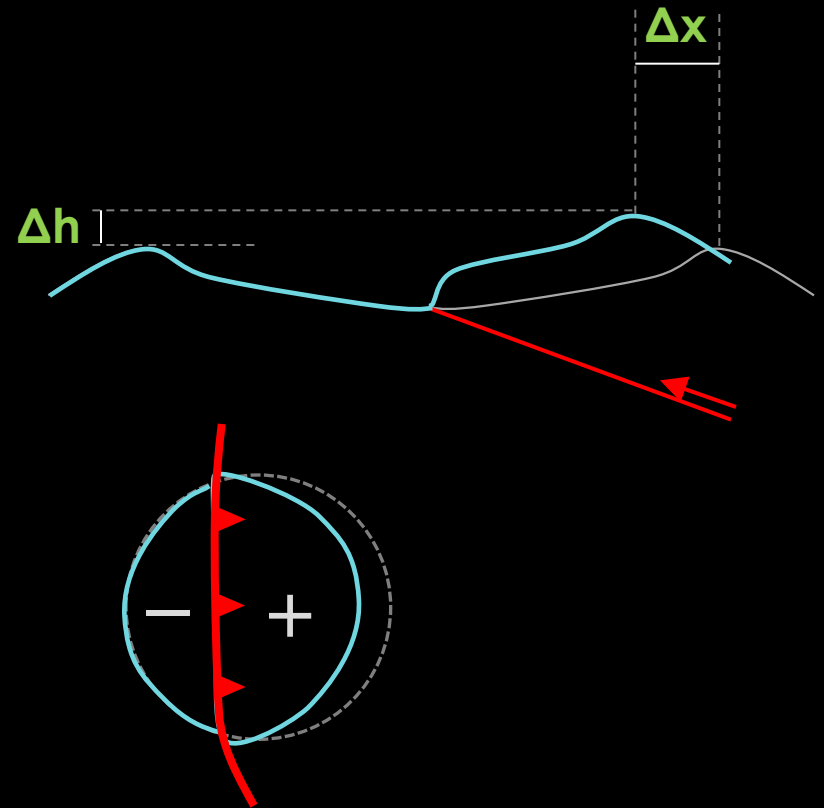
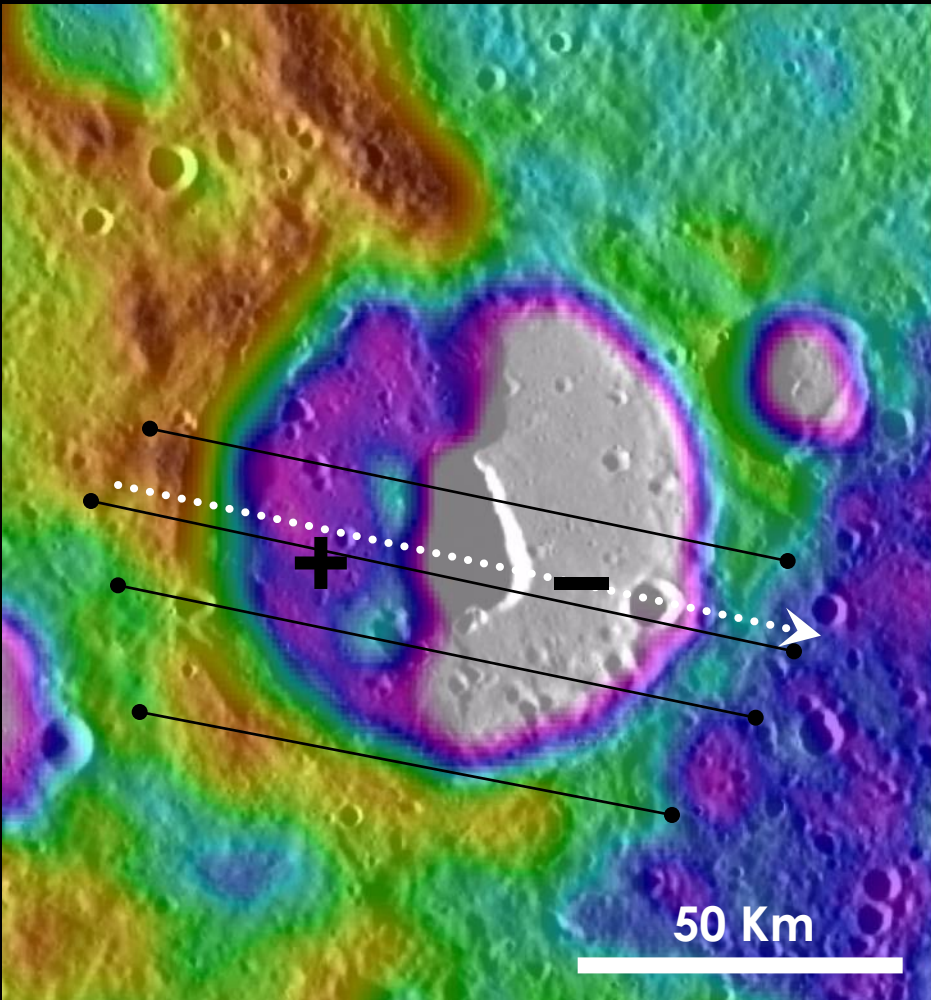
oblique-slip

$$\Phi = 0^\circ / 180^\circ$$

→

strike-slip

## STEREOGRAPHIC PROJECTION !!



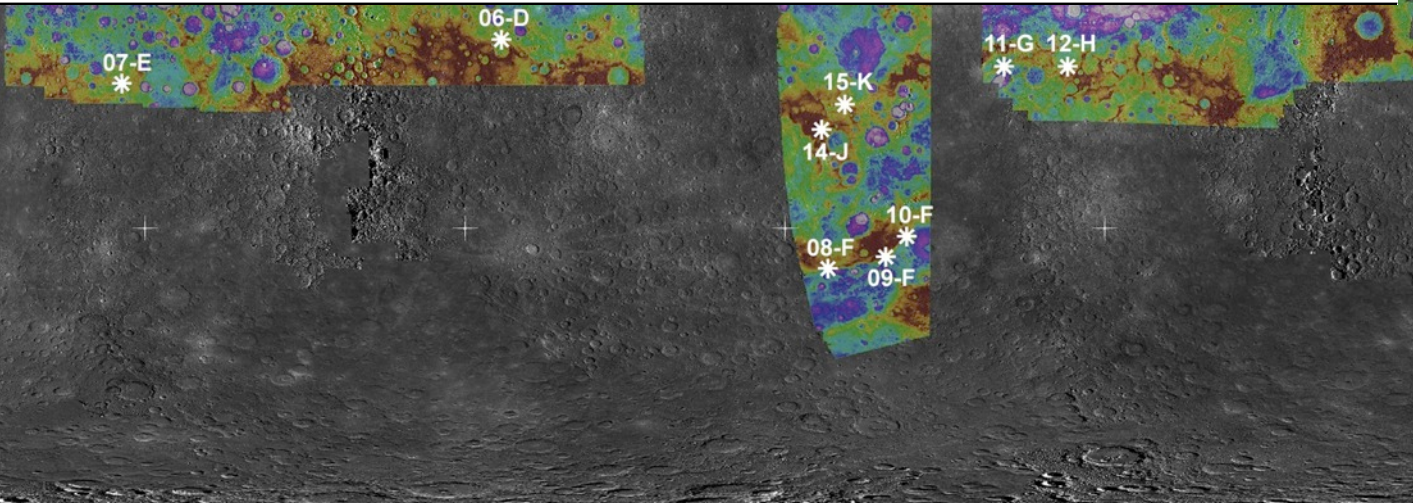
**Height** is measured preferably **on rims** to avoid floor's morphological complications e.g. central peaks, peak ring ...

$$\Delta h = h_{\max} - h_{\min}$$

# RESULTS

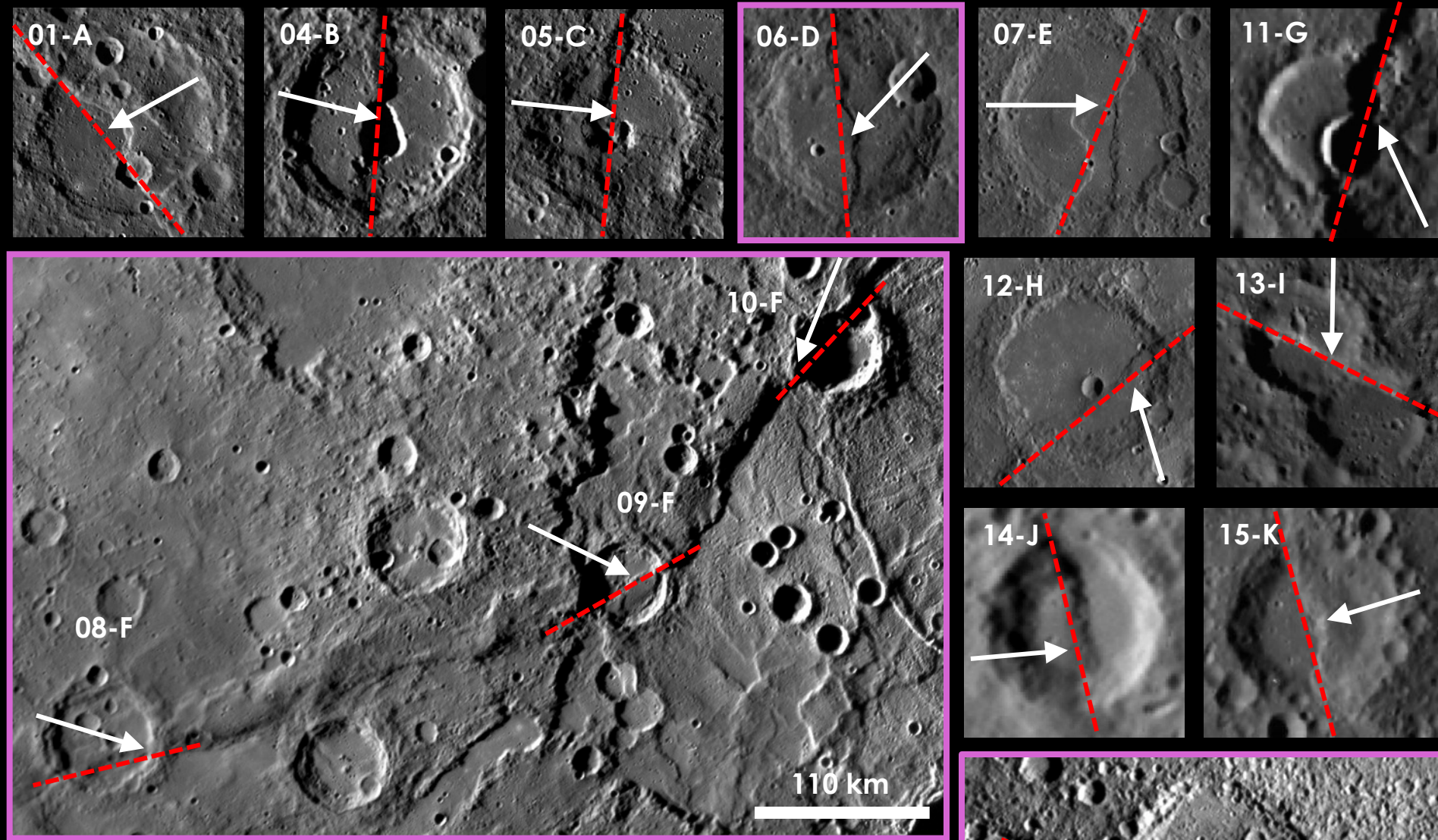
## [ fault slip data ]

| Crater              | Lon.<br>(dd) | Lat.<br>(dd) | Diameter<br>(km) | $\Delta x^a$<br>(km) | $\Delta h$<br>(km) | n | $\sigma \Delta h$<br>(km) | trend <sup>b</sup> | plunge | $\sigma$ plunge | strike <sup>c</sup> | $\delta$ | $\sigma \delta$ | $\varphi^b$ | $\lambda$ | $\sigma \lambda$ | D<br>(km) | $\sigma D$<br>(km) |
|---------------------|--------------|--------------|------------------|----------------------|--------------------|---|---------------------------|--------------------|--------|-----------------|---------------------|----------|-----------------|-------------|-----------|------------------|-----------|--------------------|
| 01-A <sup>d</sup>   | -52.5        | 58.2         | 109.90           | 4.14                 | 2.43               | 6 | 0.25                      | 241°               | 30°    | 4°              | 323°                | 31°      | 4°              | 82°         | 83°       | 10°              | 4.80      | 0.70               |
| 02-A <sup>d</sup>   | -55.0        | 58.9         | 18.27            | 1.19                 | 1.53               | 1 | 0.14                      | 218°               | 52°    | 4°              | 297°                | 53°      | 4°              | 79°         | 83°       | 7°               | 1.94      | 0.20               |
| 03-A <sup>d</sup>   | -52.3        | 57.5         | 22.13            | 1.43                 | 1.25               | 1 | 0.14                      | 236°               | 41°    | 4°              | 333°                | 42°      | 4°              | 97°         | 95°       | 9°               | 1.90      | 0.26               |
| 04-B <sup>d</sup>   | -29.6        | 27.1         | 87.30            | 4.52                 | 1.14               | 4 | 0.22                      | 104°               | 14°    | 3°              | 185°                | 14°      | 3°              | 81°         | 81°       | 14°              | 4.66      | 1.29               |
| 05-C <sup>d</sup>   | -34.0        | 49.4         | 98.57            | 3.96                 | 1.42               | 3 | 0.20                      | 96°                | 20°    | 3°              | 183°                | 20°      | 3°              | 87°         | 87°       | 14°              | 4.20      | 0.88               |
| 06-D                | 6.9          | 5.3          | 64.79            | 1.89                 | 0.77               | 4 | 0.14                      | 223°               | 22°    | 4°              | 356°                | 29°      | 8°              | 133°        | 129°      | 12°              | 2.04      | 0.50               |
| 07-E                | -64.4        | -3.0         | 107.98           | 4.44                 | 0.69               | 3 | 0.18                      | 90°                | 9°     | 2°              | 199°                | 9°       | 3°              | 109°        | 109°      | 15°              | 4.50      | 1.67               |
| 08-F                | 68.1         | -37.9        | 79.73            | 3.07                 | 1.89               | 4 | 0.16                      | 107°               | 32°    | 3°              | 263°                | 57°      | 16°             | 156°        | 141°      | 7°               | 3.60      | 0.46               |
| 09-F                | 78.8         | -35.5        | 59.70            | 2.93                 | 1.47               | 5 | 0.34                      | 116°               | 26°    | 6°              | 235°                | 30°      | 7°              | 119°        | 116°      | 10°              | 3.27      | 0.99               |
| 10-F                | 82.9         | -31.7        | 55.51            | 3.96                 | 0.93               | 6 | 0.22                      | 158°               | 13°    | 3°              | 216°                | 15°      | 5°              | 58°         | 59°       | 11°              | 4.07      | 1.41               |
| 11-G                | 101.2        | 0.2          | 16.63            | 1.87                 | 0.54               | 1 | 0.14                      | 335°               | 16°    | 4°              | 12°                 | 26°      | 10°             | 37°         | 40°       | 10°              | 1.94      | 0.68               |
| 12-H                | 113.1        | 0.2          | 85.83            | 4.43                 | 0.53               | 5 | 0.22                      | 343°               | 7°     | 3°              | 55°                 | 7°       | 3°              | 72°         | 72°       | 13°              | 4.46      | 2.59               |
| 13-I <sup>d</sup>   | -61.5        | 54.6         | 20.38            | 1.67                 | 0.33               | 1 | 0.14                      | 181°               | 11°    | 5°              | 292°                | 12°      | 5°              | 111°        | 111°      | 15°              | 1.71      | 0.98               |
| 14-J                | 66.9         | -11.6        | 32.14            | 0.82                 | 0.79               | 1 | 0.14                      | 85°                | 44°    | 6°              | 161°                | 45°      | 6°              | 76°         | 80°       | 10°              | 1.13      | 0.23               |
| 15-K                | 71.3         | -6.9         | 32.33            | 2.39                 | 0.40               | 1 | 0.14                      | 253°               | 10°    | 3°              | 343°                | 10°      | 3°              | 90°         | 90°       | 14°              | 2.43      | 1.16               |
| 16-L <sup>d,e</sup> | -28.2        | 39.9         | 15.01            | 1.08                 | 0.39               | 3 | 0.14                      | 96°                | 20°    | 7°              | 167°                | 21°      | 7°              | 71°         | 72°       | 14°              | 1.15      | 0.54               |

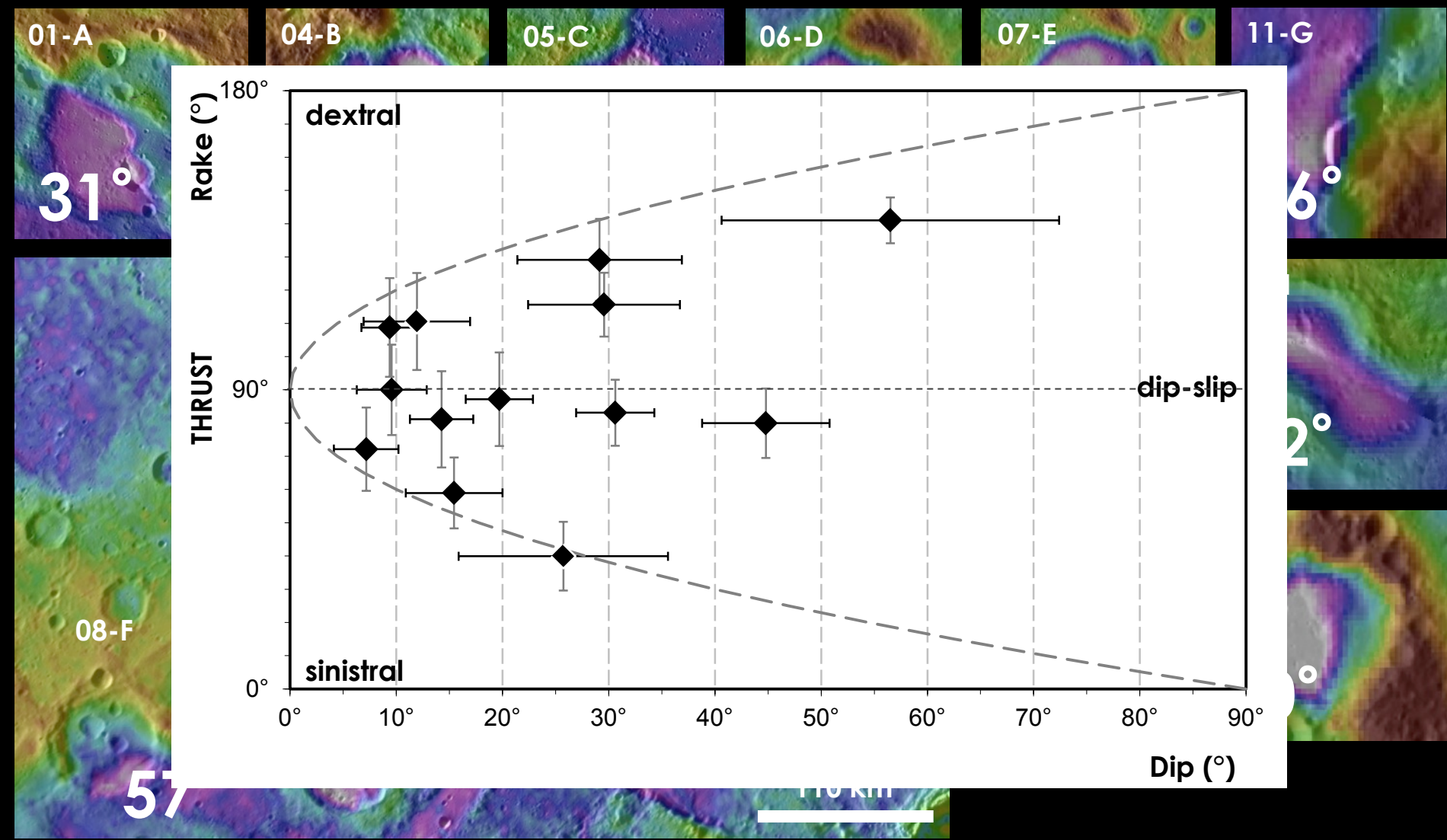


Stereo DTM Preusker et al. (2011)

Global mosaic v9 © NASA/JHUAPL/CIW



Most of the craters are  
cross-cut by oblique faults



**True dip angles:**  
 $7^\circ < \theta < 57^\circ$  wide range

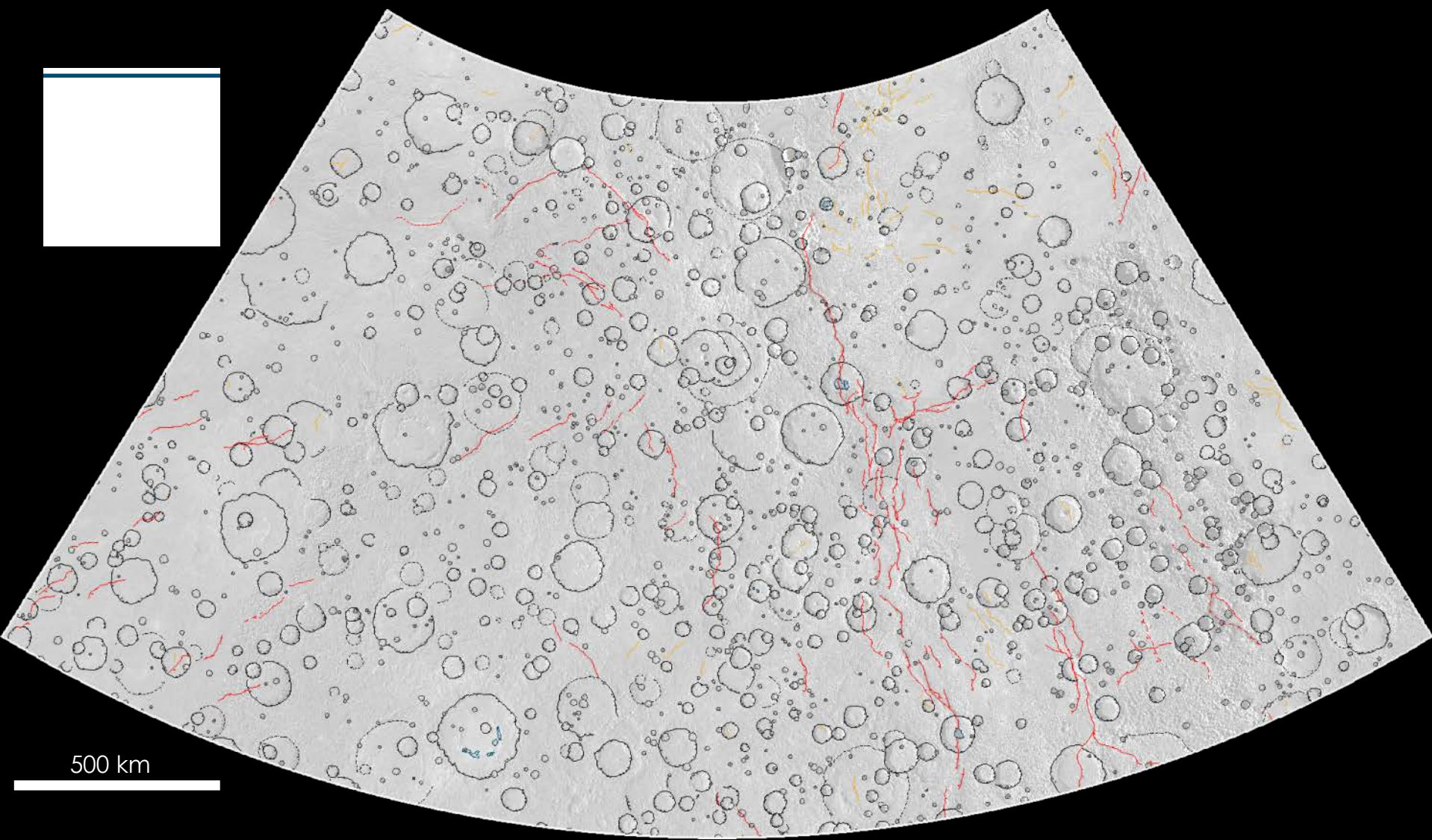
hypothetical dips:  
 $25^\circ < \theta < 35^\circ$

+ strike-slip comp.  
+ high dip



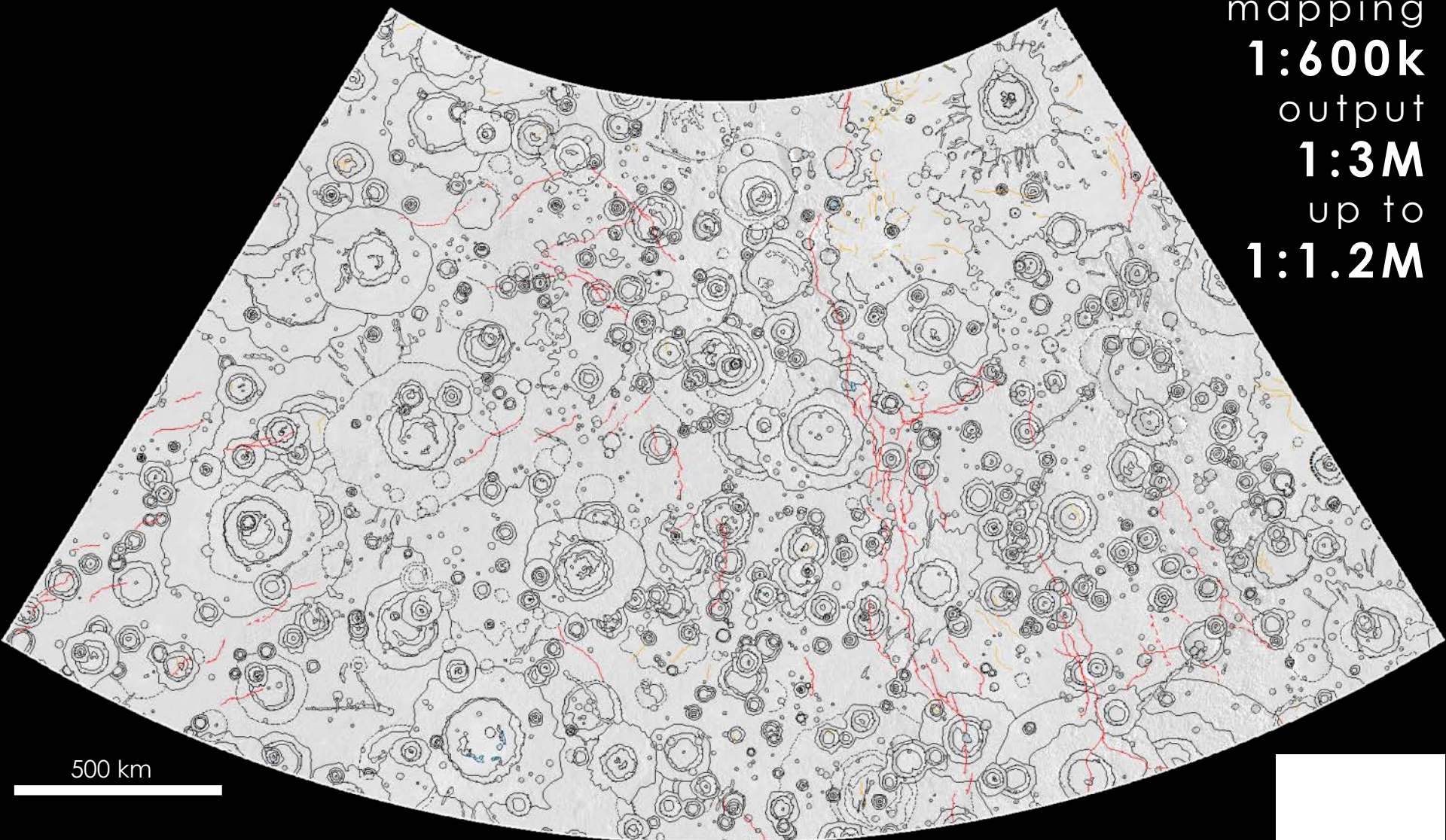
# RESULTS

[ geology ]



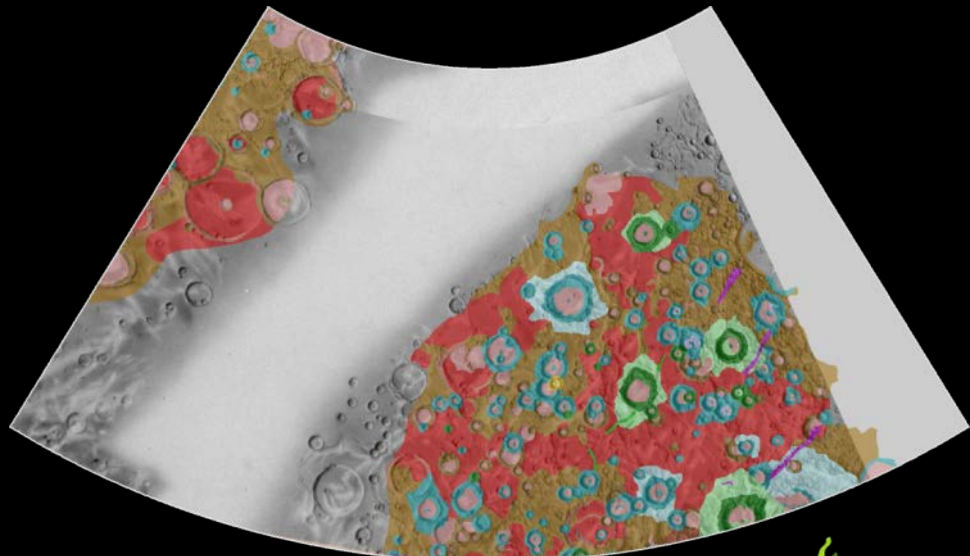
500 km

mapping  
**1:600k**  
output  
**1:3M**  
up to  
**1:1.2M**

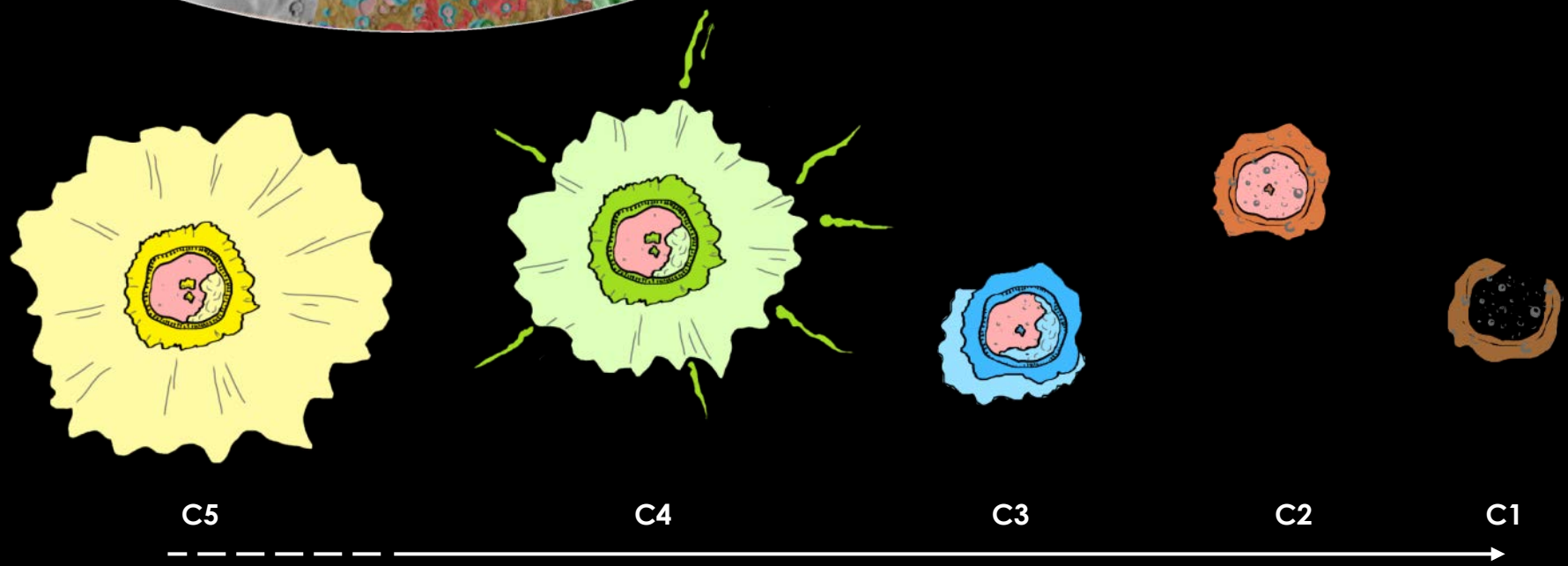


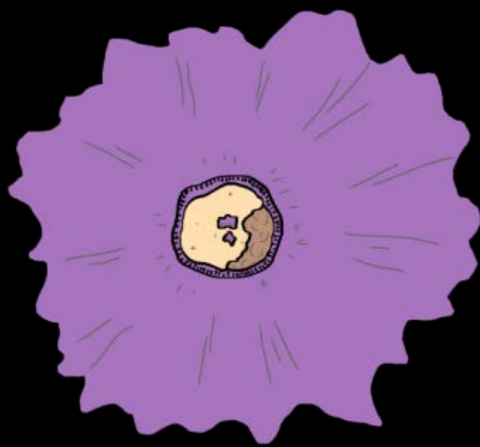
500 km

McGill & King (1983)

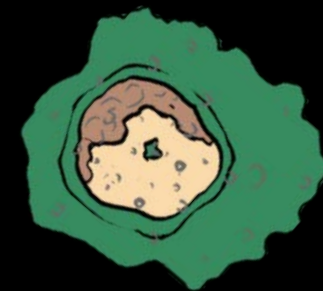


| PLAINS MATERIALS | CRATER AND BASIN MATERIALS |                 |                 |                 |                 |
|------------------|----------------------------|-----------------|-----------------|-----------------|-----------------|
|                  | c <sub>5</sub>             | cp <sub>5</sub> | cf <sub>5</sub> | cr <sub>5</sub> | cs <sub>4</sub> |
| ps               |                            |                 |                 |                 |                 |
| psi              |                            |                 |                 |                 |                 |
| pc               |                            |                 |                 |                 |                 |
| pi               |                            |                 |                 |                 |                 |
| c <sub>4</sub>   | cp <sub>4</sub>            | cf <sub>4</sub> | cr <sub>4</sub> | cs <sub>4</sub> |                 |
| c <sub>3</sub>   | cp <sub>3</sub>            | cf <sub>3</sub> | cr <sub>3</sub> |                 |                 |
| c <sub>2</sub>   | cp <sub>2</sub>            |                 |                 |                 |                 |
| c <sub>1</sub>   |                            |                 |                 |                 |                 |
|                  |                            |                 |                 |                 | cs <sub>4</sub> |

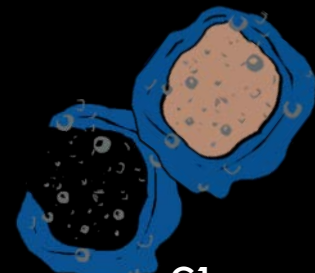




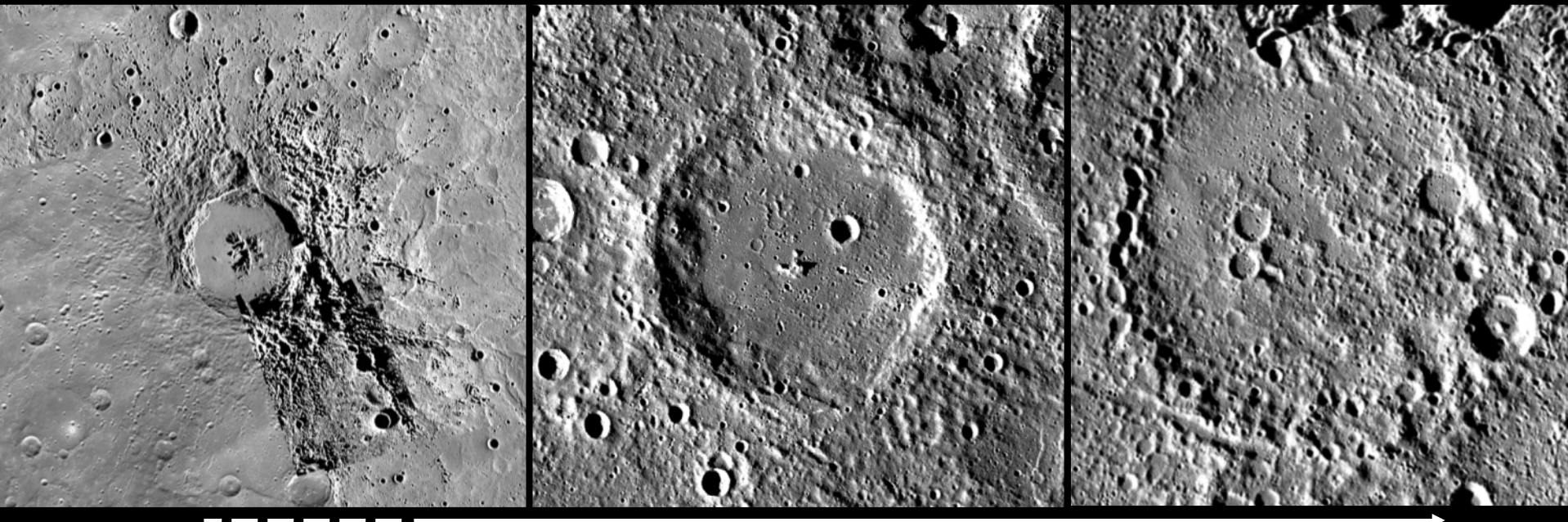
C3

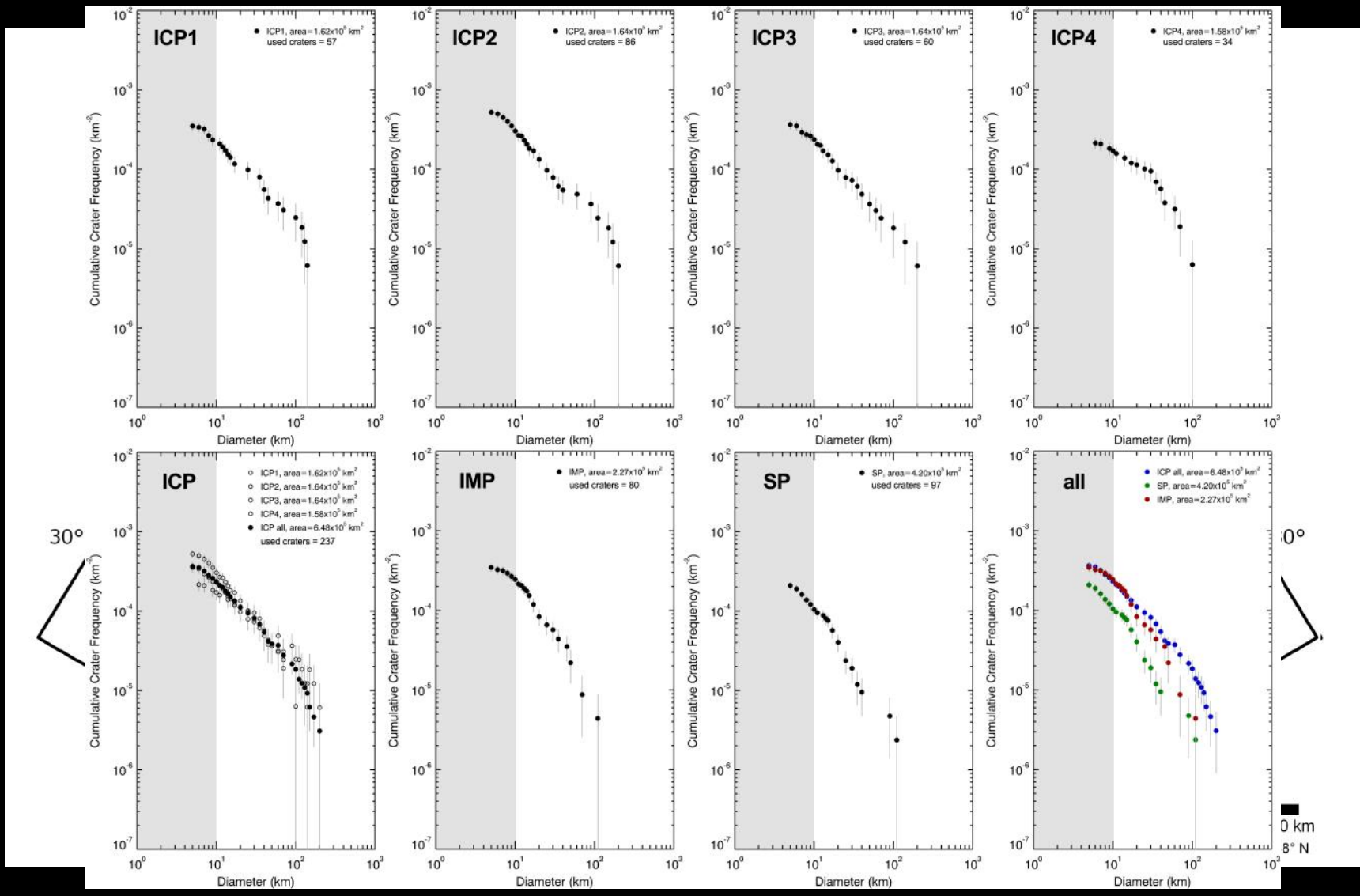


C2



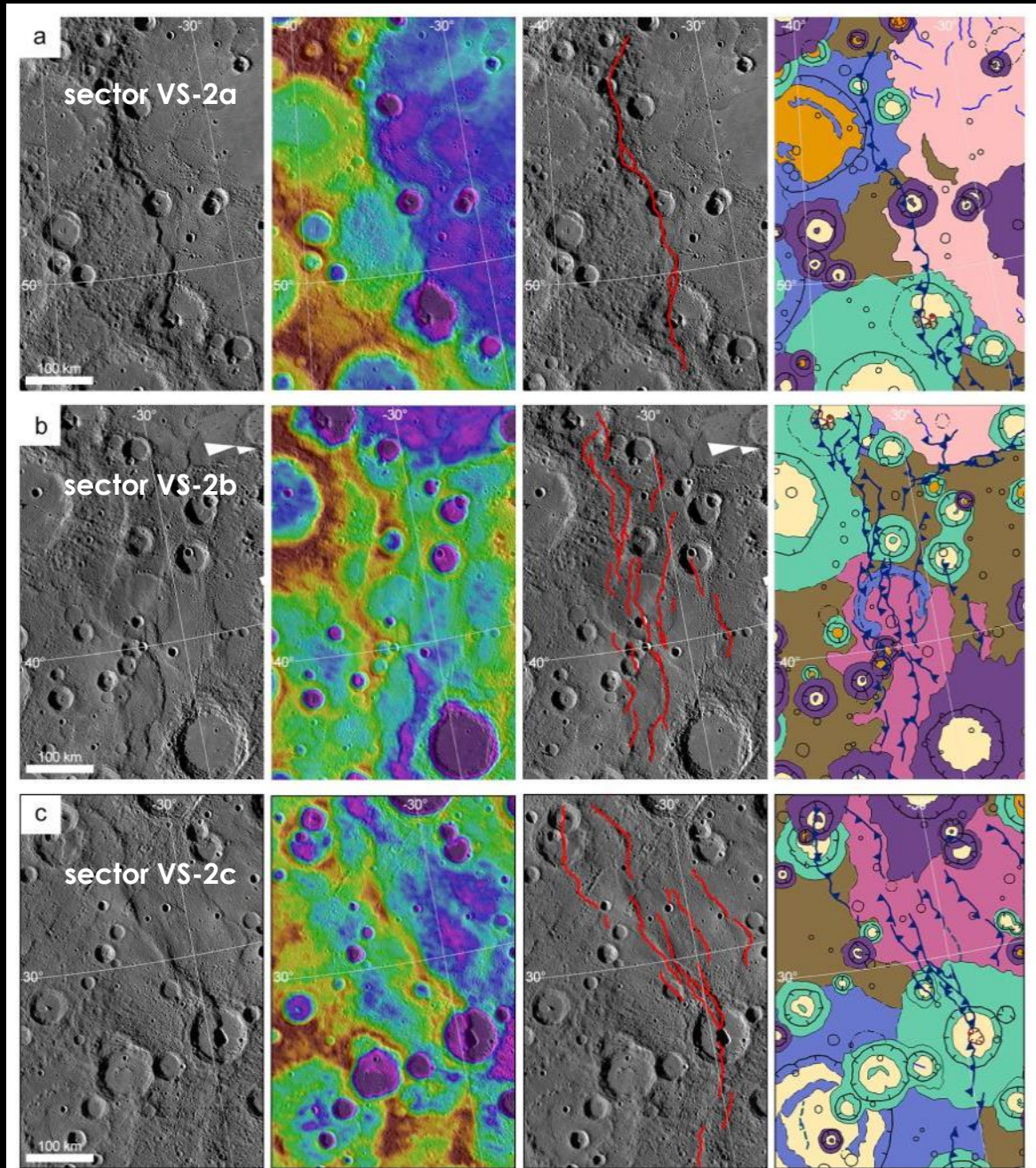
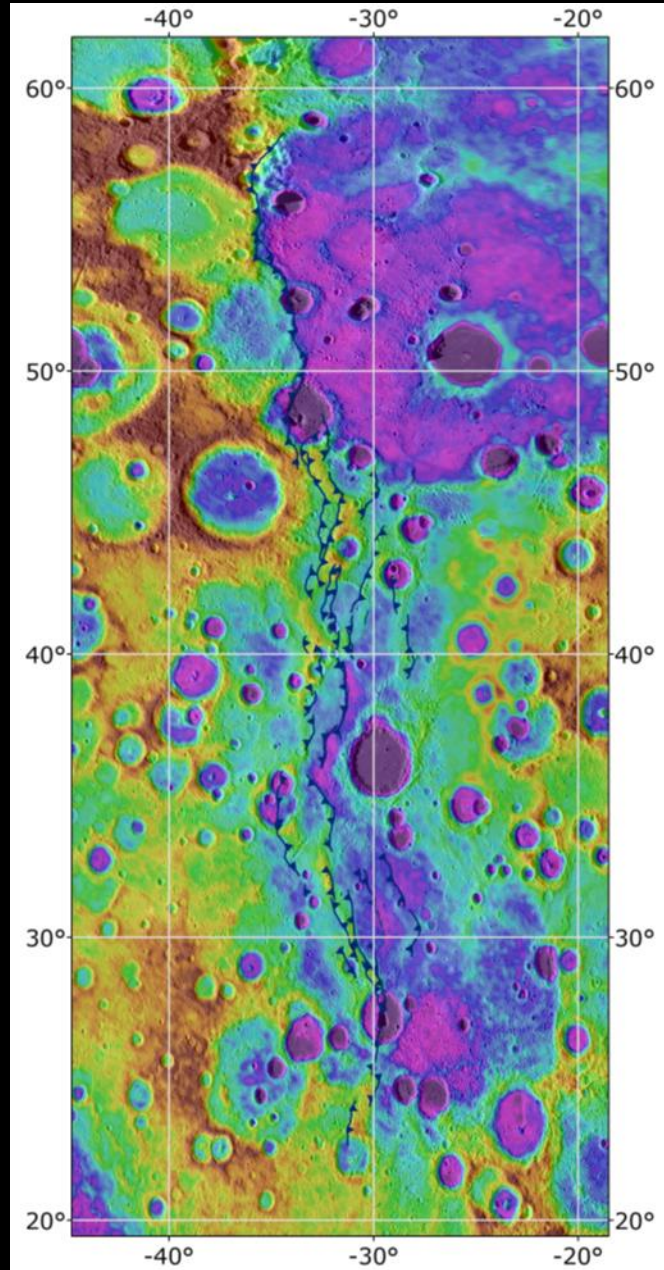
C1

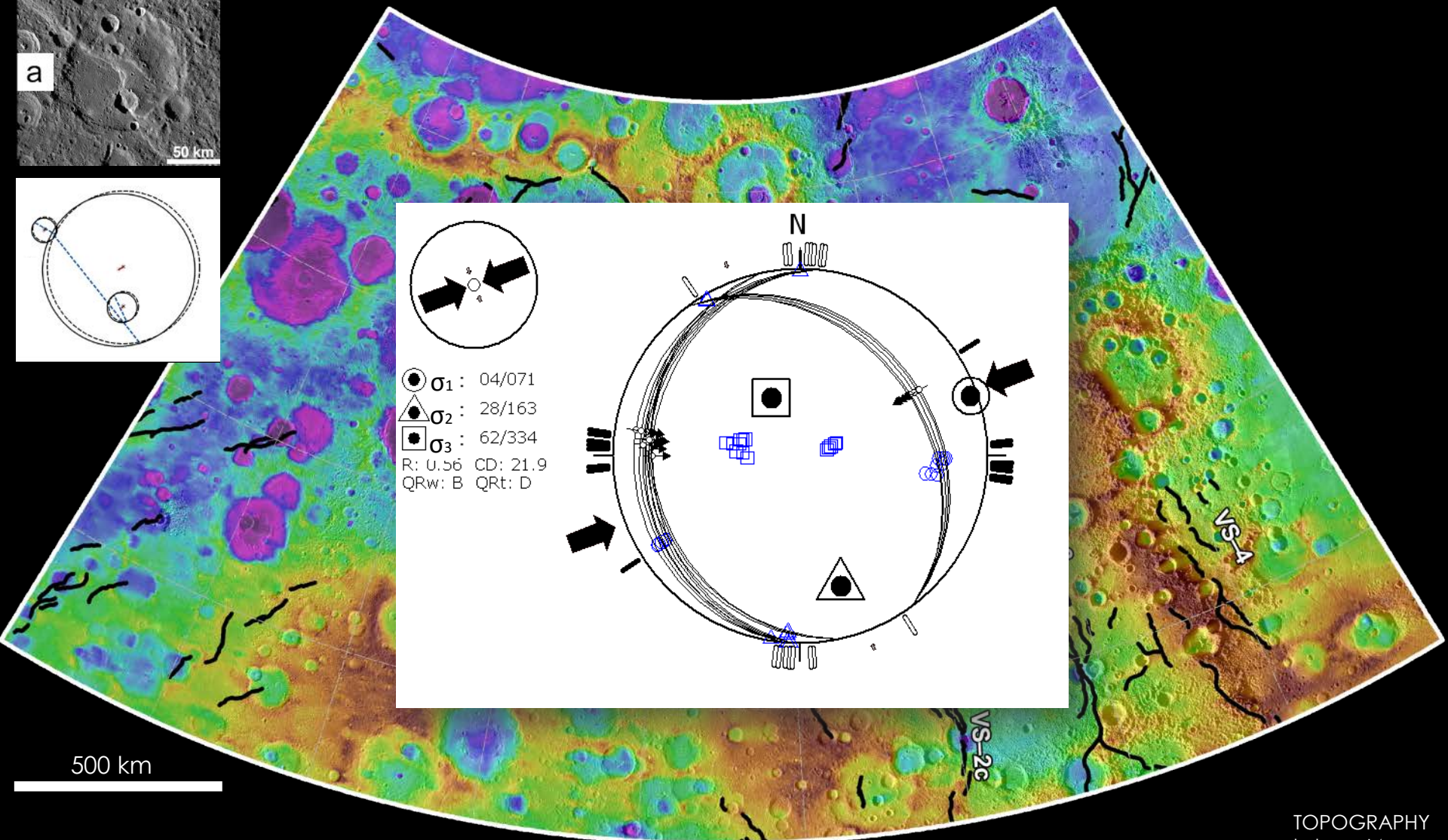
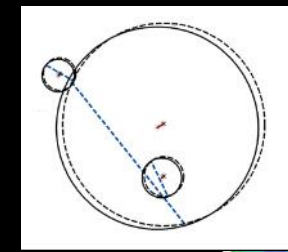
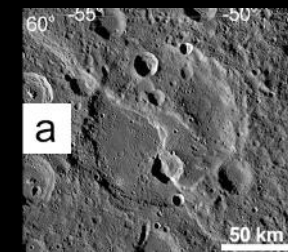




# RESULTS

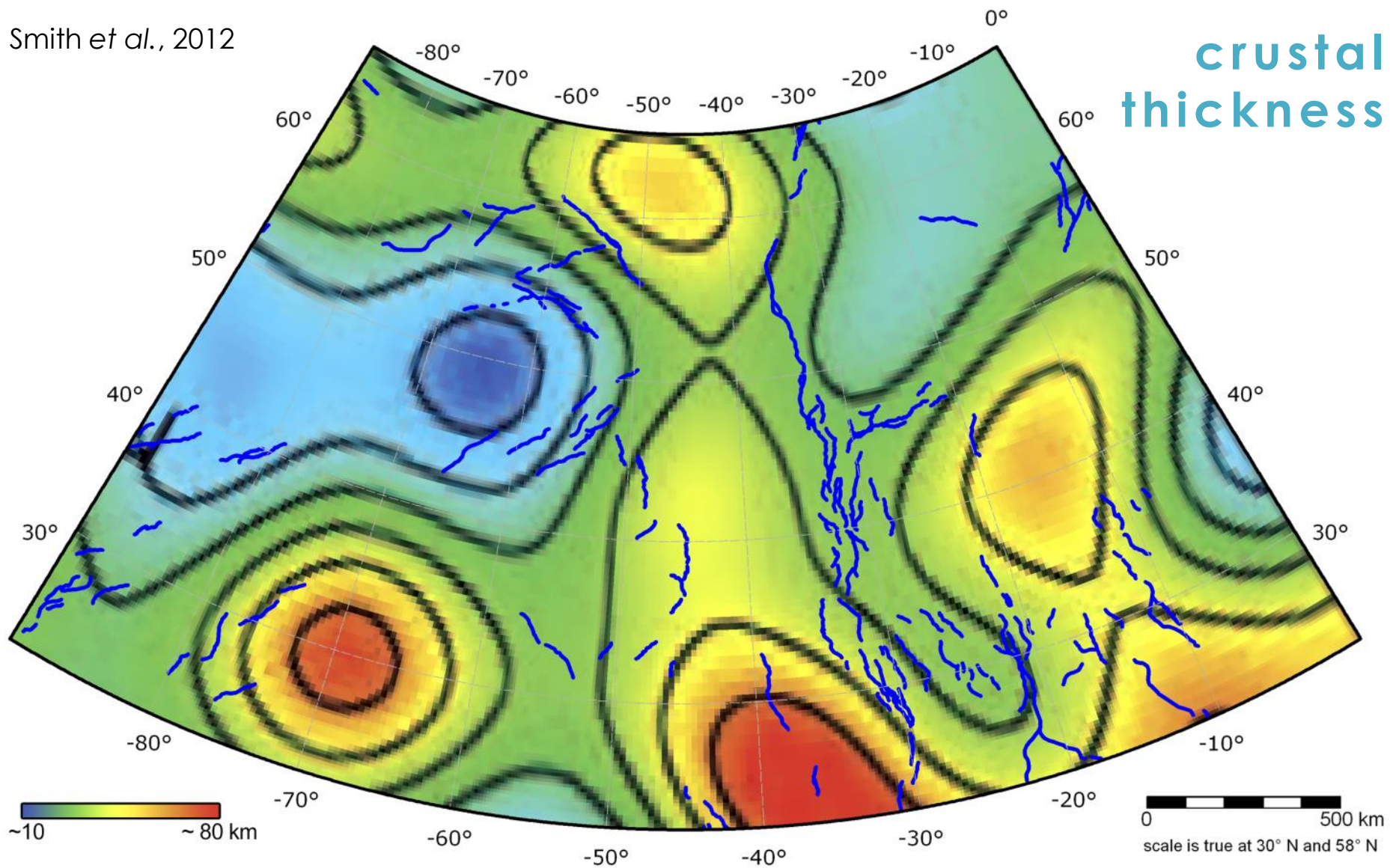
## [ structural framework ]



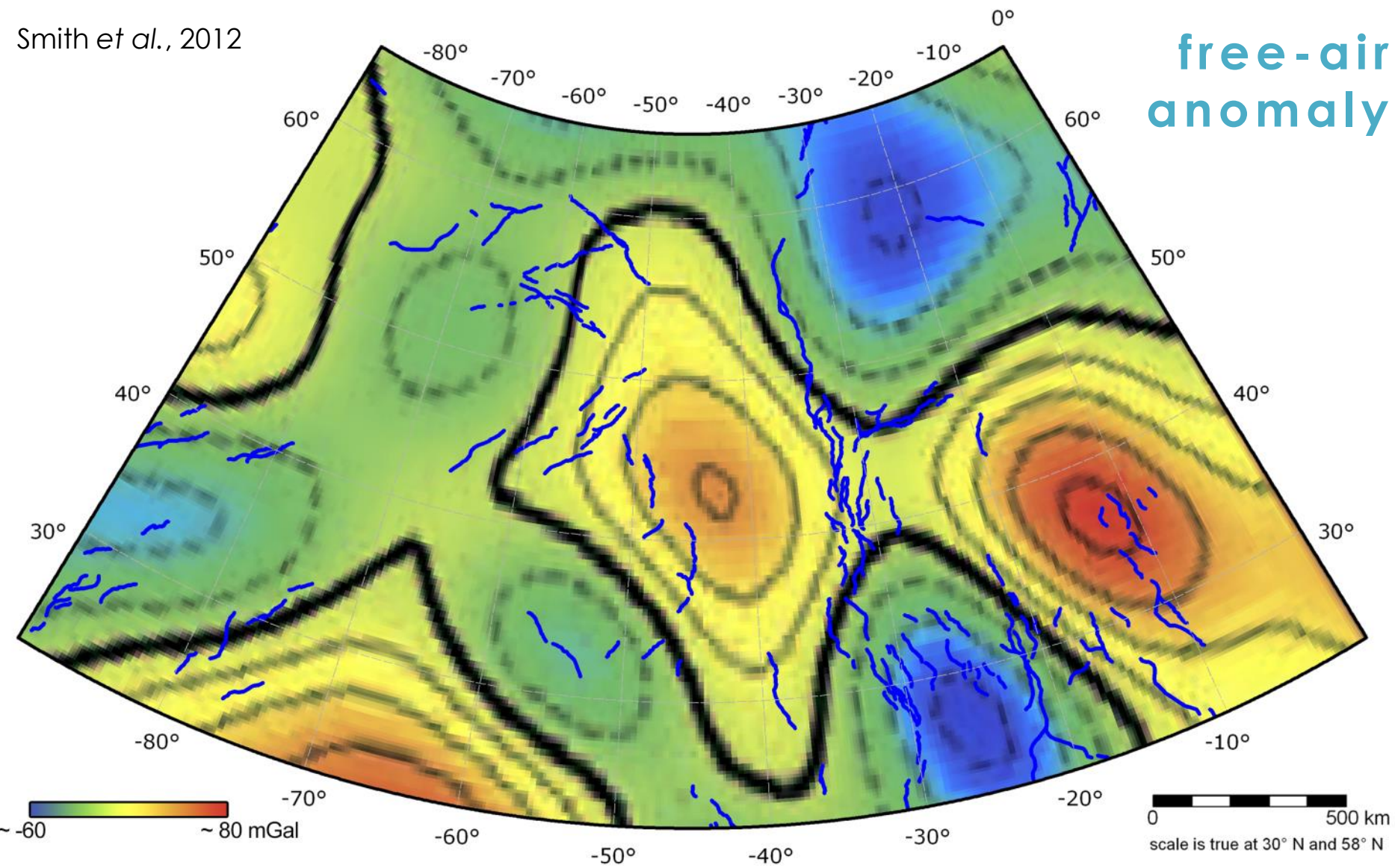


TOPOGRAPHY  
hdem\_64  
© NASA

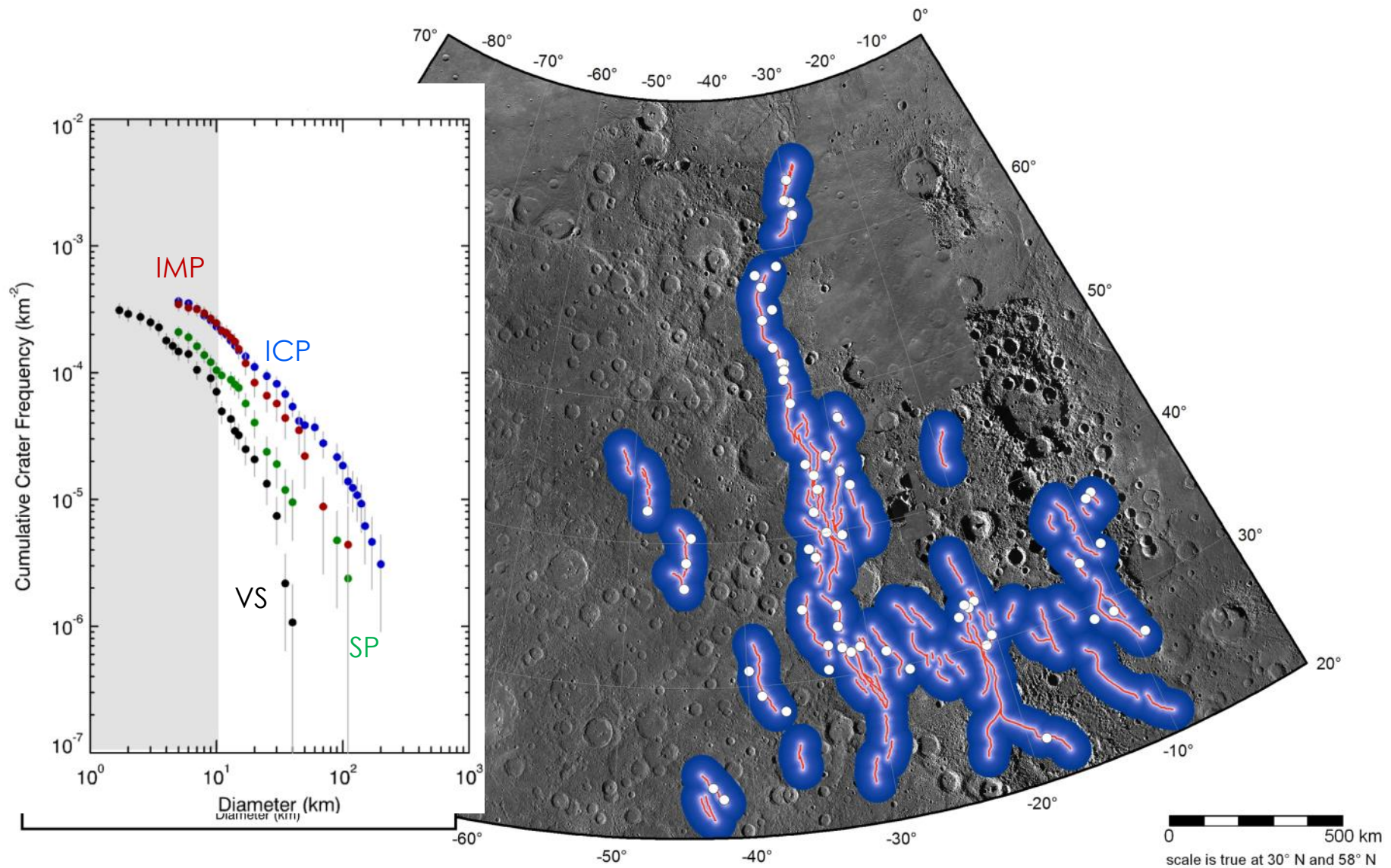
Smith et al., 2012



Smith et al., 2012



# buffered crater counting



# CONCLUSIONS

- ▶ the **Victoria quadrangle** has now a **complete geologic map**
- ▶ a **tectonic fault-free pop-up** is present between the V-E-A array and the antithetic Carnegie thrust
- ▶ probable **mantle discontinuities** could explain the V-E-A bulge **N-S alignment**
- ▶ it is possible that **two stages of deformation** acted on this area
- ▶ **tectonics** and **fault segmentation** are most probably related to **volcanic activity**
- ▶ first time that **fault slip data** and **strain inversion** are estimated on **remote-sensed faults!**

# OPEN ISSUES & FUTURE WORK

- ▶ what is the cause of Hermean thrust **shallow angles** ? → **overthrusts** ?
- ▶ which targets will be chosen for the future ESA/JAXA BepiColombo mission ?  
→ **GEOLOGIC GLOBAL COVERAGE CAN HELP !!**



THANK  
YOU

[valentina.galluzzi@iaps.inaf.it](mailto:valentina.galluzzi@iaps.inaf.it)



This research was supported by the Italian Space Agency (ASI) within the SIMBIOSYS project (ASI-INAF agreement n. I/022/10/0).